01 Feb 1969

Further Investigation of Light Gage Steel Forms As Reinforcement for Concrete Slabs

C. E. Ekberg Jr.

R. M. Schuster

Max L. Porter

ENGINEERING
RESEARCH

ENGINEERING
RESEARCH

ENGINEERING
RESEARCH

ENGINEERING
RESEARCH

ENGINEERING
RESEARCH

PROGRESS REPORT NO. 5

FURTHER INVESTIGATION OF LIGHT GAGE STEEL FORMS AS REINFORCEMENT FOR CONCRETE SLABS

C. E. Ekberg, Jr.
R. M. Schuster
M. L. Porter

February 1, 1969

Report to American Iron and Steel Institute

ERI-395
Project 760-S

ENGINEERING RESEARCH INSTITUTE
IOWA STATE UNIVERSITY AMES

FIGURES

		Page
Fig. 1.	Illustration of vertical test.	18
Fig. 2.	Illustration of beam test.	19
Fig. 3.	Typical cross section of form I.	20
Fig. 4.	Typical form assembly for vertical pushout tests.	21
Fig. 5.	Typical form assembly for beam tests.	21
Fig. 6.	Failed beam specimens for casting numbers 8, 9, and 10 using 18-gage steel form I.	22
Fig. 7.	Failed beam specimens for casting numbers 11 and 12 using 18-gage steel form I.	23
Fig. 8.	Failed beam specimens for casting numbers 8 and 9 using 22-gage smooth steel form I.	23
Fig. 9.	Failed beam specimens for casting numbers 8, 9, and 10 using 22-gage steel form I.	24
Fig. 10.	Failed beam specimens for casting numbers 11 and 12 using 22-gage steel form I.	25
Fig. 11.	Applied load, P, vs deflection for embedment lengths of 12, 18, 24, and 34 in. (each curve is the average of 5 tests) for beams consisting of 18-gage steel form I.	26
Fig. 12.	Applied load, P, vs deflection for embedment length of 12, 18, 24, and 34 in. (each curve is the average of 5 tests) for beams consisting of 22-gage steel form I.	27
Fig. 13.	Applied moment, M, vs deflection for beams consisting of 18- and 22-gage steel form I.	28
Fig. 14.	Applied moment, M, vs embedment length, L', for beams consisting of 18- and 22-gage steel form I.	29
Fig. 15.	Applied moment, M, vs form thickness for embedment lengths of 12, 18, 24, and 34 in. for form I.	30
Fig. 16.	Form stresses, f_{scp} and f_{scb}, vs embedment length, L', for beams consisting of 18- and 22-gage steel form I.	31

		Page
Fig. 17.	Form stresses, f_{scp} and f_{scb}, and form load, F_u, vs form thickness for embedment lengths, L', of 12, 18, 24, and 34 in. for form I.	32
Fig. 18.	Shear, V_u, vs embedment length, L', for beams consisting of 18- and 22-gage steel form I.	33
Fig. 19.	Shear, V_u, vs form thickness for embedment length, L', of 12, 18, 24, and 34 in. for form I.	34
Fig. 20.	Mechanical bond stresses, u_b and u_b', vs embedment length, L', for beams consisting of 18- and 22-gage steel form I.	35
Fig. 21.	Typical embedment lengths for pushout specimens.	36
Fig. 22.	Typical vertical pushout failure for form I.	36
Fig. 23.	Mechanical bond stresses, u_p and u_p', vs embedment length, L', for beams consisting of 18- and 22-gage steel form I.	37
Fig. 24.	Mechanical bond stresses, u_b, u_b', u_p, and u_p', vs form thickness for beam and pushout specimens of embedment lengths of 12, 18, 24, and 34 in. for form I.	38
Fig. 25.	Ratio, $R_{f_{sc}}$, vs embedment length, L', for specimens consisting of 18- and 22-gage steel form I.	39
Fig. 26.	Ratio, $R_{f_{sc}}$, vs form thickness for embedment lengths of 12, 18, 24 and 34 in. for form I.	40
Fig. 27.	Ratio, R_u, vs embedment length, L', for specimens of 18- and 22-gage steel form I.	41
Fig. 28.	Ratio, R_u, vs form thickness for embedment lengths of 12, 18, 24, and 34 in. for form I.	42

TABLES

		Page
Table 1.	Typical properties of form I.	44
Table 2.	Summary of concrete properties used in casting specimens. (See Table 3 in August report.)	45
Table 3.	Computed quantities needed to obtain M_{ab}, M_{ac}, and M_c in Table 5.	46
Table 4.	Computed quantities needed to obtain M_u' in Table 5.	47
Table 5.	Tabulation of design and ultimate moments. (See Table 1 in August report.)	48
Table 6.	Experimental test results from beams using 18- and 22-gage steel form I. (See Table 12 in August report.)	49
Table 7.	Design and ultimate moment comparisons for beams using 18- and 22-gage steel form I. (See Table 39 in August report.)	51
Table 8.	Experimental and design mechanical bond comparisons for beams. (See Table 38 in August report.)	53
Table 9.	Experimental results for pushout tests. (See Tables 4 and 8 in August report.)	54
Table 10.	Experimental correlation of pushout tests to beam tests. (See Table 33 in August report.)	55

INTRODUCTION

This report describes the results of tests of 40 vertical pushout specimens and 44 corresponding beam specimens. These tests followed those described in the Progress Report of Aug. 1, 1968, hereafter referred to as the August report. The need for the additional tests was to ascertain the effect of varying the gage thickness of the steel form. Secondary objectives were to ascertain the consistency of the vertical pushout test in obtaining data for evaluation of the ultimate strength of form-reinforced slabs and to supplement existing data on the effect of varying the embedment length, L' (shear span), of the steel form.

The tests contained in this report were performed and analyzed in a manner very similar to that of the August report. Therefore, the text of this report is brief and is supplemented with frequent reference to the August report.

NOMENCLATURE

Before delving into the specimens tested, a brief summary of the nomenclature is given. Two types of tests were conducted, namely:

- Type V = vertical pushout test
- Type B = beam test.

An illustration of the vertical pushout test is given in Fig. 1 (for all figures given in this report, see Appendix B), and an illustration of the beam test in Fig. 2. The order of the designations used in each type of test specimen is given next by showing an example for each; however, for a general review of all nomenclature used throughout this report, see Appendix A.

Example of designation for vertical pushout test:

VI 18 - 12 - 8 - 11

where: V = vertical pushout specimen

I = light-gage steel form, which in this case is form I

18 = gage thickness of steel form

12 = embedment length, L', in inches

8 = casting number

11 = number of days elapsed from casting to testing.

Example of designation for beam specimen:

BI 22 S - 18 - 9 - 20

where: B = beam test specimen

I = form I was used

22 = gage thickness of steel form

S = smooth form I was used (this letter is omitted if a regular form I was used)

18 = shear span (embedment length), L', in inches

9 = casting number

20 = number of days elapsed from casting to testing.

SPECIMENS, TEST PROCEDURE, AND TEST EQUIPMENT

All specimens cast were composed of form I containing embossments, except for the smooth specimens, of either 18- or 22-gage thickness. Typical dimensions for this form are shown in Fig. 3. Note in the August report that those specimens cast with form I were composed only of forms of 20-gage thickness. Typical properties of the steel form I used are given in Table 1 (see Appendix C). In all cases for specimens in this report, the light-gage steel form was free of dirt, grease or oil at the time of casting.

Concrete forms for the test units used prefabricated steel forms supplied by the Economy Forms Co., Des Moines, Iowa. Figure 4 shows a typical form assembly for a vertical pushout test, and Fig. 5 shows a typical form assembly for a beam specimen.

Five castings were made for the specimens described in this report. All concrete was made with Type I portland cement, supplied by Ames Ready-Mix Concrete, Inc. A complete tabulation of the concrete properties used in these 5 castings, casting numbers 8 through 12, is given in Table 2. The average compressive strength, f'_c, given in Table 2 was obtained from standard 6 x 12 in. cylinders at about the time of testing of the specimens, shown by the age given in the various tables. Fabrication, casting and curing of all specimens were as described on pages 16 and 17 of the August report.

The 40 vertical test specimens consisted of 5 specimens each of embedment lengths, L', of 12, 18, 24 and 34 in. for both the 18- and 22-gage steel forms. Each vertical specimen was tested by clamping the top block to hold it against failure while testing the bottom block.

The August report indicates that in previous work, both the top and bottom blocks were tested; however, it was decided to test only the bottom blocks for this investigation. The vertical test specimens were tested by placing a 20-ton hydraulic jack between the upper and lower blocks (Fig. 1), pushing them apart, and recording the ultimate load at failure.

For each of the 40 pushout specimens there was a corresponding beam specimen of the same embedment length, L', and gage thickness. In addition, 4 beam specimens were cast with smooth forms. The beam specimens were tested by loading at constant head speed up to the ultimate, recording the centerline deflection in increments of 200 lb, recording the ultimate load, and noting the crack patterns and location of the failure crack. All beam specimens were tested under two-point loading (Fig. 2), except those of embedment length, L', of 34 in. which were tested under a single concentrated load applied at midspan.

TEST RESULTS AND ANALYSIS

Beam Specimens

Like the form I beam specimens described in the August report, the beam specimens discussed here also failed by lack of composite action between the concrete and steel form. Figures 6 and 7 show the failed beam specimens for the 5 castings (8 — 12) using 18-gage steel form I. Figure 8 shows the failed specimens using the smooth (without the embossments) steel form I. Figures 9 and 10 show the failed beam specimens consisting of a 22-gage steel form I. Note that the failure crack in nearly all of the above beams occurs at, or near, one of the load points of the beam.

For analyzing the beam results, computational aids were prepared to help in computing the design moments, M_{ab}, (based on allowable steel stress of 20,000 psi to bottom fiber of beam) M_{ac}, (based on allowable steel stress of 20,000 psi to the centroid of the steel form), and M_c, (based on an allowable concrete stress of $f_c = 0.45\ f'_c$. These aids are given in Table 3. Similarly, aids given in Table 4, were prepared in computing the expected ultimate moment, M'_u, of the beam. A complete tabulation of the design and ultimate moments is given in Table 5 for the beams using 18- and 22-gage steel forms.

The actual experimental moments, and the computed experimental steel form stresses (based on a cracked section) at the centroidal axis, f_{scb}, and at the bottom fiber, f_{sb}, are tabulated in Table 6. A comprehensive comparison of the experimental moments given in Table 6, to the computed design and ultimate moments given in Table 5, are tabulated as ratios in Table 7.

The load-deflection behavior for beams consisting of 18- and 22-gage steel forms are shown on Figs. 11 and 12 respectively. The difference in the stiffness characteristics between the 18- and 22-gage for each embedment length, L', may be observed by comparing these two figures.

Some behavioral characteristics in the beams tested can be seen in Figs. 13, 14, and 15. Figure 13 indicates the deflection variation with corresponding applied moment for both the beams consisting of the 18- and 22-gage steel forms. The variation of moment as a function of embedment length is shown in Fig. 14. A good indication of the stiffness pattern may be obtained by looking at the moment, M_u, as a function of the gage number, shown in Fig. 15.

The variation of form stress given in Table 6 (as mentioned above) is shown as a function of embedment length, L', in Fig. 16. As can be seen from Fig. 16, there is only a slight increase in the form stress as the embedment length increases. Correspondingly, the variation of form stress as a function of gage number is given in Fig. 17 (the top series of curves). In this later series of curves, there is, as expected, a definite increase in form stress as the thickness of the steel form decreases. The only exception is one test for the 20 gage which was tested significantly older (55 days) than the other specimens; hence, age may have a detrimental effect possibly due to shrinkage effects. However, more testing is needed to ascertain any effects of age.

The effects of the shear force acting on the embedment length (shear span) are shown as a function of the various embedment lengths in Fig. 18. Note the decrease in shear load capacity with an increase in the shear span for each of three gages (18, 20, and 22). The relationship between shear capacity and gage thickness of steel form is shown in Fig. 19.

As was done in connection with the August report, the mechanical bond stresses were computed for the beams tested. This mechanical bond stress is based on either the total bonded area or on the effective bonded area. The total bonded perimeter, for computing total bonded area, is based on the entire contact perimeter, neglecting the embossments. The computation of effective bonded area is based on the perimeter found by taking the sum of projected lengths of the embossments on the cross section. The tabulation of these mechanical bond stresses is shown in Table 8. Based on the manufacturer's catalog-recommended value of 40 psi as the allowable bond stress, the ratios of the actual experimental computed value for both the total and effective mechanical bond stresses to the allowable are also shown in Table 8. The relationship of these bond stresses as a function of embedment length, L', is shown in Fig. 20. As can be seen in Fig. 20, the mechanical bond stresses decrease as the embedment length increases.

Pushout Tests

To correspond to each of the shear span lengths, L', of the beams, a corresponding pushout specimen was formed with a corresponding embedment length equal to that of the shear span. A sample of each of these embedment lengths for the pushout tests is shown in Fig. 21. Each of the pushout specimens failed by loss of composite action of the steel form with the concrete block. Figure 22 shows a typical failure of a vertical pushout specimen using form I.

A complete tabulation of the experimental results for the pushout tests is shown in Table 9. The form load, F_u, taken by each of the steel forms comprising the pushout test was found by dividing the jack load by two. As was the case with the beams, the mechanical bond stresses, u_p and u'_p, were obtained by dividing the force in the form by the bonded area (either effective or total areas). Figure 23 shows the variation of total and effective mechanical bond stresses as a function of embedment length, L'. The variation of the bond stresses as a function of the gage number is shown in Fig. 24. In Fig. 24, the comparison of the magnitudes of pushout results and the beam results can be seen for the mechanical bond stresses.

Figures 16 and 17 indicate how the pushout form stress, f_{scp}, varies with embedment length, L' and gage number. Also evident is the comparison of the magnitudes of the pushout form stress, f_{scp}, and the beam form stress, f_{scb}, for each of the embedment lengths tested.

Correlation of Pushout to Beam Results

Here a brief comparison of the pushout to beam results is made. A tabulation was made of the ratios, $R_{f_{sc}}$, for pushout form stress, f_{scp}, to beam form stress, f_{scb}, and the ratios, R_u, for pushout mechanical bond stress, u_p, to beam mechanical bond stress, u_b. These ratios are given in Table 10.

The relationships of the ratio of $R_{f_{sc}}$ as a function of embedment length, L', and gage number are shown in Figs. 25 and 26, respectively. Figure 25 shows the consistency of the pushout to beam relationship for the embedment lengths tested. This same consistency can be seen by looking at the ratio, R_u, as a function of embedment length, L', as seen in Fig. 27. The relationship of this ratio, R_u, as a function of gage number is then shown in Fig. 28.

CONCLUSIONS

On the basis of the tests conducted to date, the vertical push-out test appears to yield reliable results. As was observed in the August report, the specimens tested here also failed by a breakdown of the composite action of the steel form and the concrete. For the beams, in no case was the full flexural strength of the steel or concrete a primary cause of failure and hence the pushout specimens seems to give consistent results for the various embedment lengths tested.

As expected, the increased thickness of a lower gage number provides increased stiffness to the form-reinforced slab. However, the relationship is not directly proportional, as was seen in looking at the results.

Some of the behavioral conclusions are as follows:

1. The ultimate moment capacity of the form-reinforced slab increases with an increased shear span.

2. The ultimate moment capacity decreases as the steel form thickness decreases.

3. There is only a slight increase in form stress as the embedment length increases.

4. Ultimate form stress increases as the steel form thickness decreases in both the beam and pushout specimens.

5. Ultimate pushout form load, F_u, decreases with a decrease in steel form thickness.

6. Ultimate shear capacity decreases as the shear span increases.

7. Ultimate shear capacity tends to decrease with a decrease in steel form thickness.

8. Ultimate mechanical bond stress tends to decrease with an increased embedment length.

9. Ultimate mechanical bond stress tends to decrease as the steel form thickness decreases.

10. The ratio of form stresses, $R_{f_{sc}}$, is constant over the range of the embedment lengths tested.

11. The ratio of form stresses, $R_{f_{sc}}$, tends to increase only slightly with a decrease in steel form thickness.

12. The ratio of mechanical bond stresses, R_u, is constant over the range of the embedment lengths tested.

13. The ratio of mechanical bond stresses, R_u, tends to increase only slightly with a decrease in steel form thickness.

ACKNOWLEDGMENTS

The authors would particularly like to thank Mr. Lynn A. Boettcher for his assistance with the experimental work and his diligence and care in reduction of data and preparation of figures. Also, thanks are due to Mr. Kenneth W. Mouw for his help in preparing this report.

APPENDIX A. GENERAL NOTATIONS

a	depth of rectangular stress block in inches as given by $A_s f_y/(0.85\ f'_c)(b)$
A_s	cross-sectional area of steel form in square inches
b	width of compression face of flexure member in inches
c	distance form neutral axis of flexure member to extreme fiber in inches
c_{sb}	distance from neutral axis of flexure member to bottom fiber of steel form in inches
c_{scb}	distance from neutral axis of flexure member to centroidal axis of steel form in inches
d	distance from extreme compression fiber to centroid of steel form in inches
d_s	depth of steel form in inches
E_c	modulus of elasticity of concrete in psi
E_s	modulus of elasticity of steel in psi
f_c	allowable strength of concrete in psi
f'_c	compressive strength of concrete in psi
f_s	allowable steel stress in psi
f_{sb}	experimental value of steel stress at bottom fiber of steel section in psi
f_{scb}	experimental value of steel stress at centroid of steel section in psi based on beam tests
f_{scp}	experimental value of steel stress at centroid of steel section in psi based on pushout tests
f_y	yield strength of steel in psi
F_u	experimental ultimate load on steel form in pounds
I_T	transformed moment of inertia of composite slab in inches to the fourth power
j	ratio of distance between centroid of compression and centroid of tension to the depth, d

k	ratio of distance between extreme compression fiber and neutral axis to the depth, d
L	length of beam specimen
L'	shear span length for beams, or embedment length for pushout specimens in inches
M	Applied moment in beam at any particular level
M_{ab}	Allowable design moment capacity of beam in foot-pounds based on depth to bottom fiber of steel form
M_{ac}	Allowable design moment capacity of beam in foot-pounds based on depth to centroid of steel form
M_c	allowable design moment capacity of beam in foot-pounds based on $f_c = 0.45\ f'_c$
M_u	experimental ultimate moment capacity of beam in foot-pounds
M'_u	calculated ultimate moment capacity of beam in foot-pounds by ACI code
n	ratio of modulus of elasticity of steel to that of concrete
p	A_s/bd
P	total applied load at any particular level
P_u	ultimate load in pounds
$R_{f_{sc}}$	ratio of pushout test form stress to beam form stress
R_u	ratio of pushout mechanical bond stress to beam mechanical bond stress
t	thickness of light-gage steel form
u_a	allowable bond stress
u_b	mechanical bond stress in psi as given by $V_u/\Sigma_o jd$ for beams
u'_b	effective mechanical bond stress in psi as given by $V_u/\Sigma'_o jd$ for beams
u_p	mechanical bond stress in psi as given by $F_u/\Sigma_o L'$ for pushout tests
u'_p	effective mechanical bond stress as given by $F_u/\Sigma'_o L'$ for pushout tests in psi

V	shear force at any point in pounds
V_u	ultimate experimental shear in pounds
$\bar{y}$	centroid of steel form from bottom fiber in inches
Σ_o	sum of total surface areas per unit length for light-gage steel form in contact with concrete in inches
Σ'_o	sum of effective surface area (acting on plate of embossments) per unit length for light-gage steel form in contact with concrete in inches. This is found by taking the sum of the projected lengths of the embossments on the cross section.

APPENDIX B. FIGURES

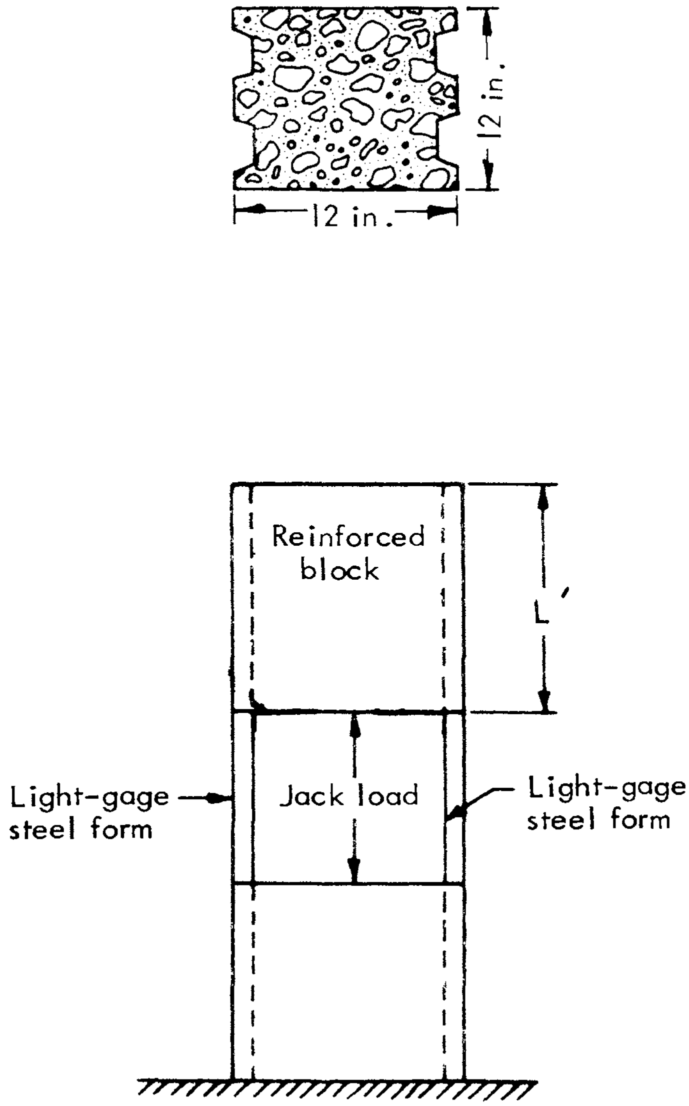

Fig. 1. Illustration of vertical test.

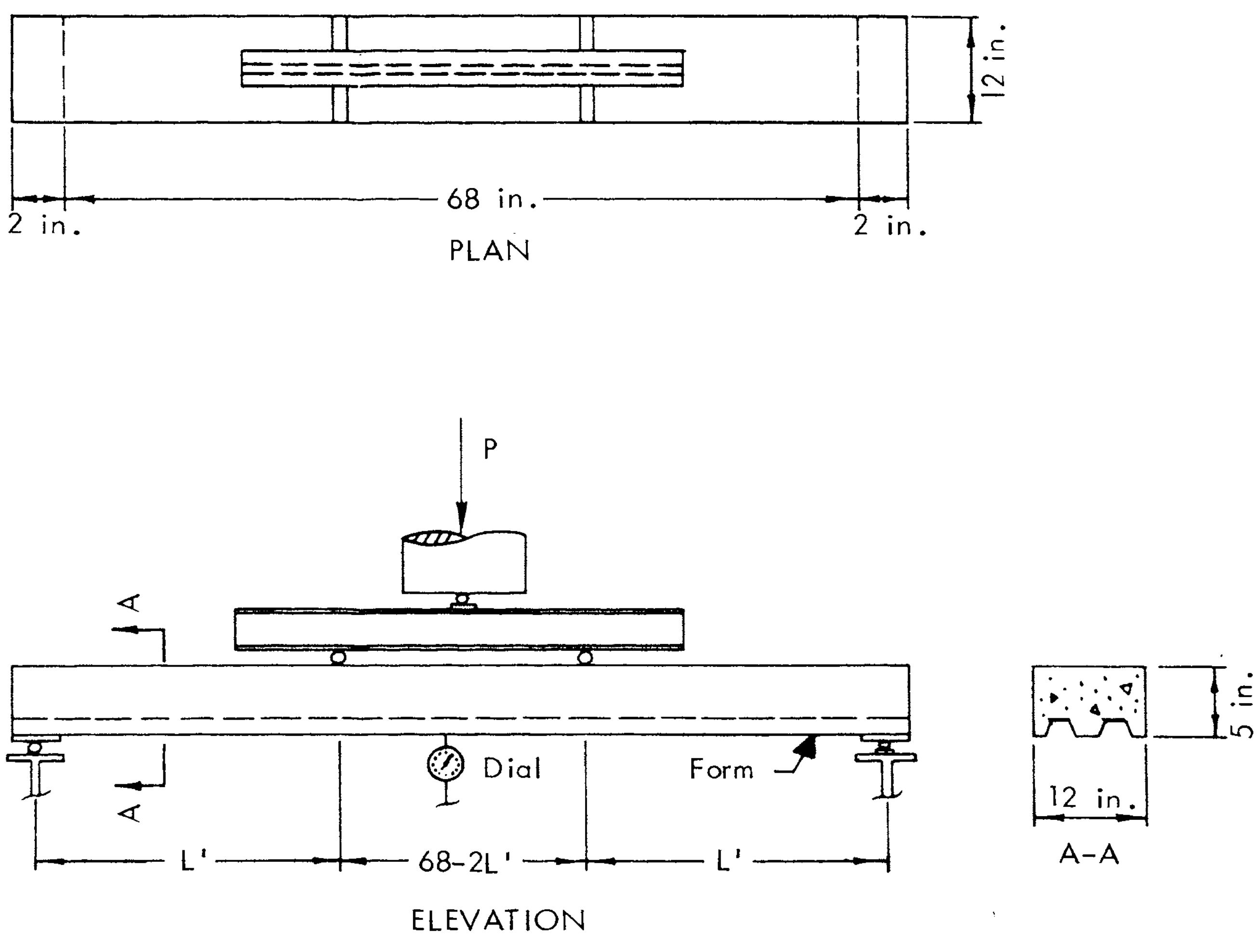

Fig. 2. Illustration of beam test.

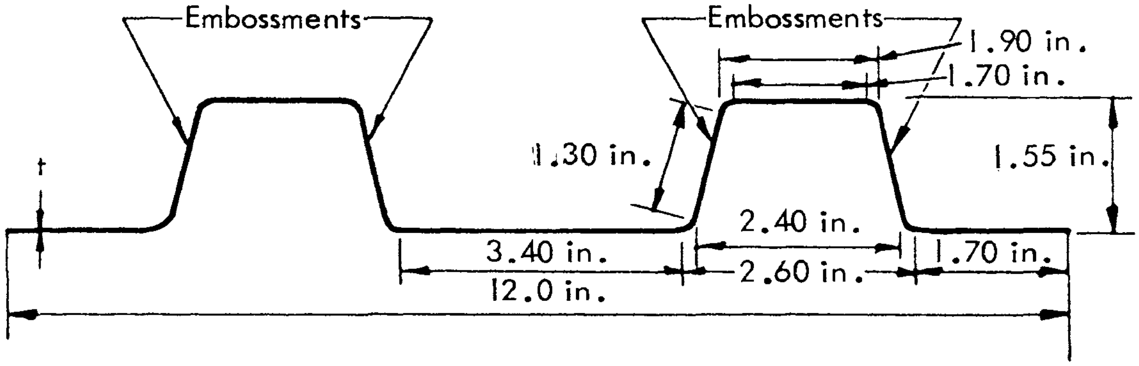

Fig. 3. Typical cross section of form I.

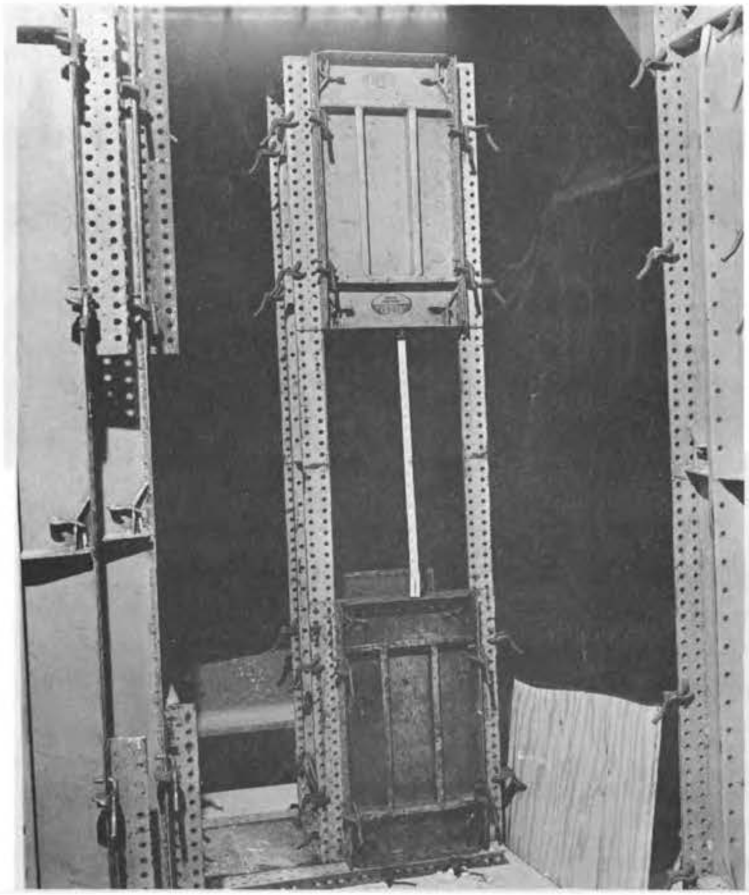

Fig. 4. Typical form assembly for vertical pushout tests.

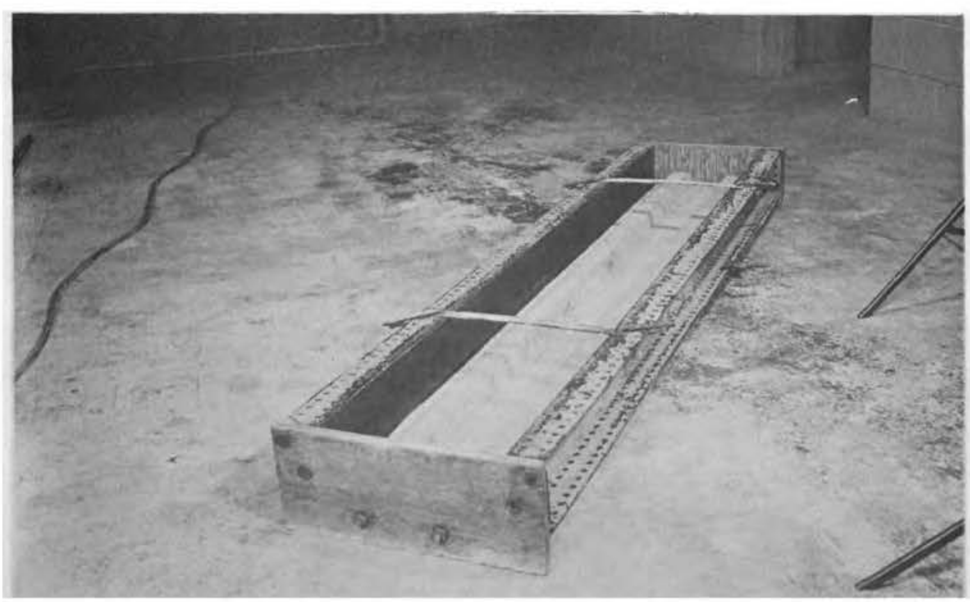

Fig. 5. Typical form assembly for beam tests.

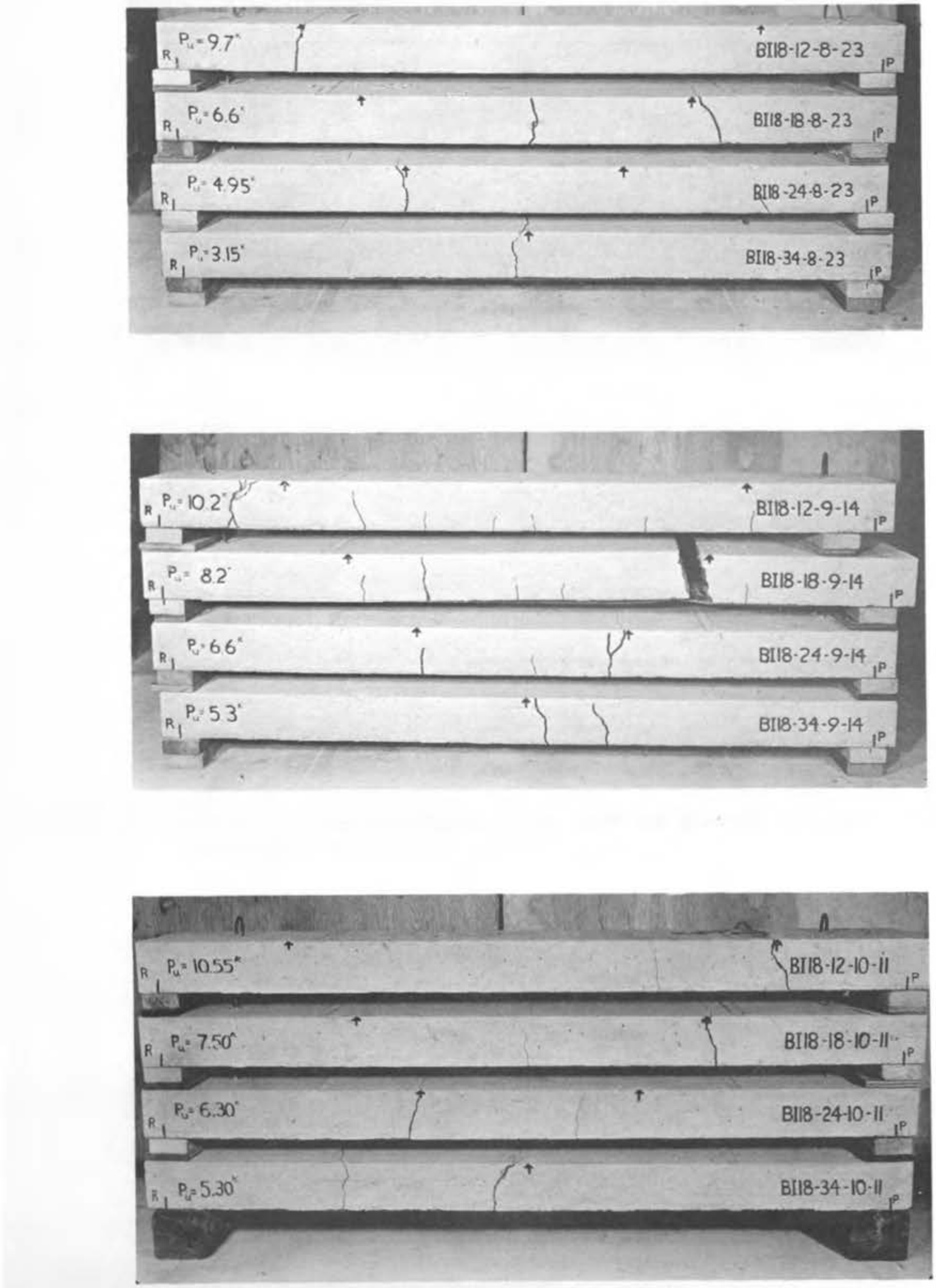

Fig. 6. Failed beam specimens for casting numbers 8, 9, and 10 using 18-gage steel form I.

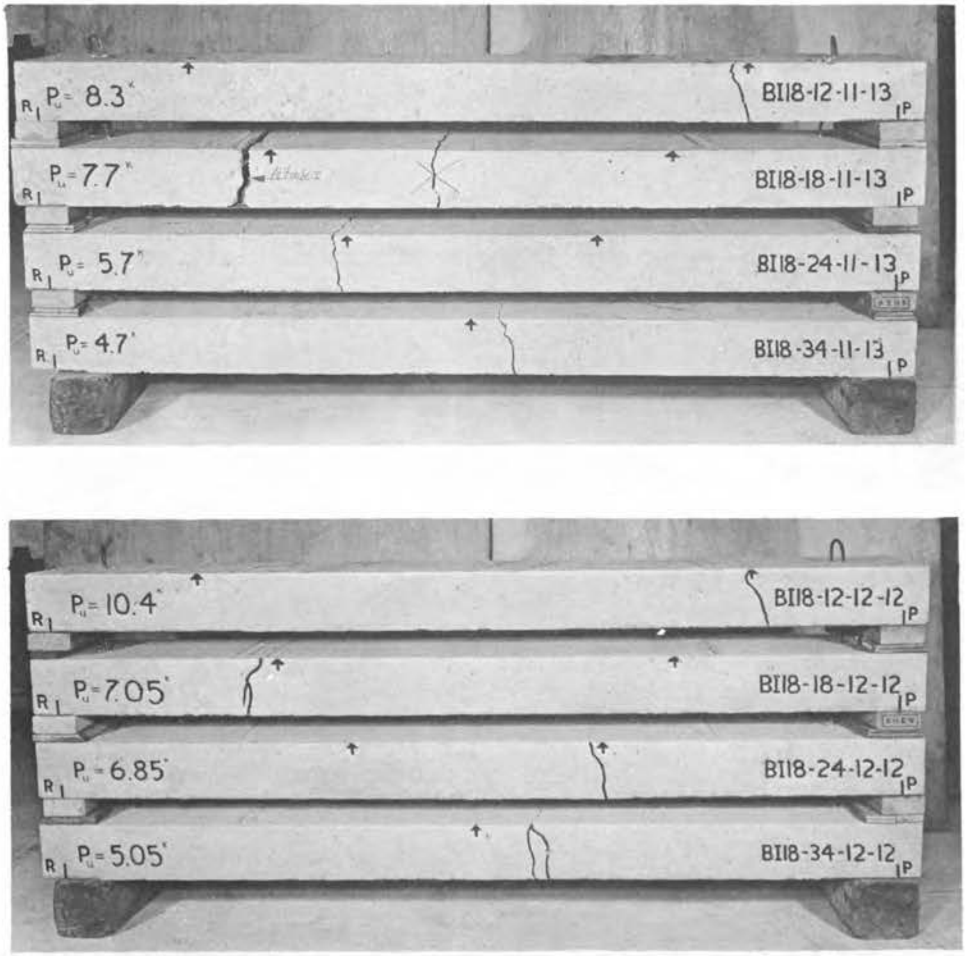

Fig. 7. Failed beam specimens for casting numbers 11 and 12 using 18-gage steel form I.

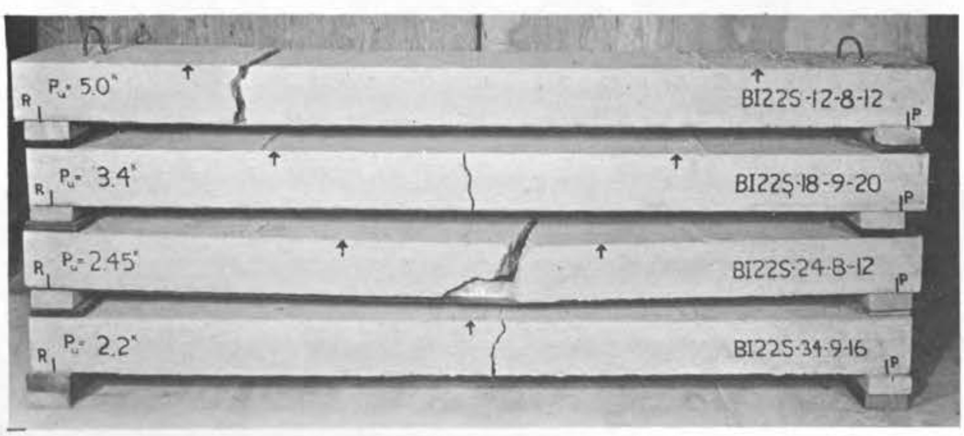

Fig. 8. Failed beam specimens for casting numbers 8 and 9 using 22-gage smooth steel form I.

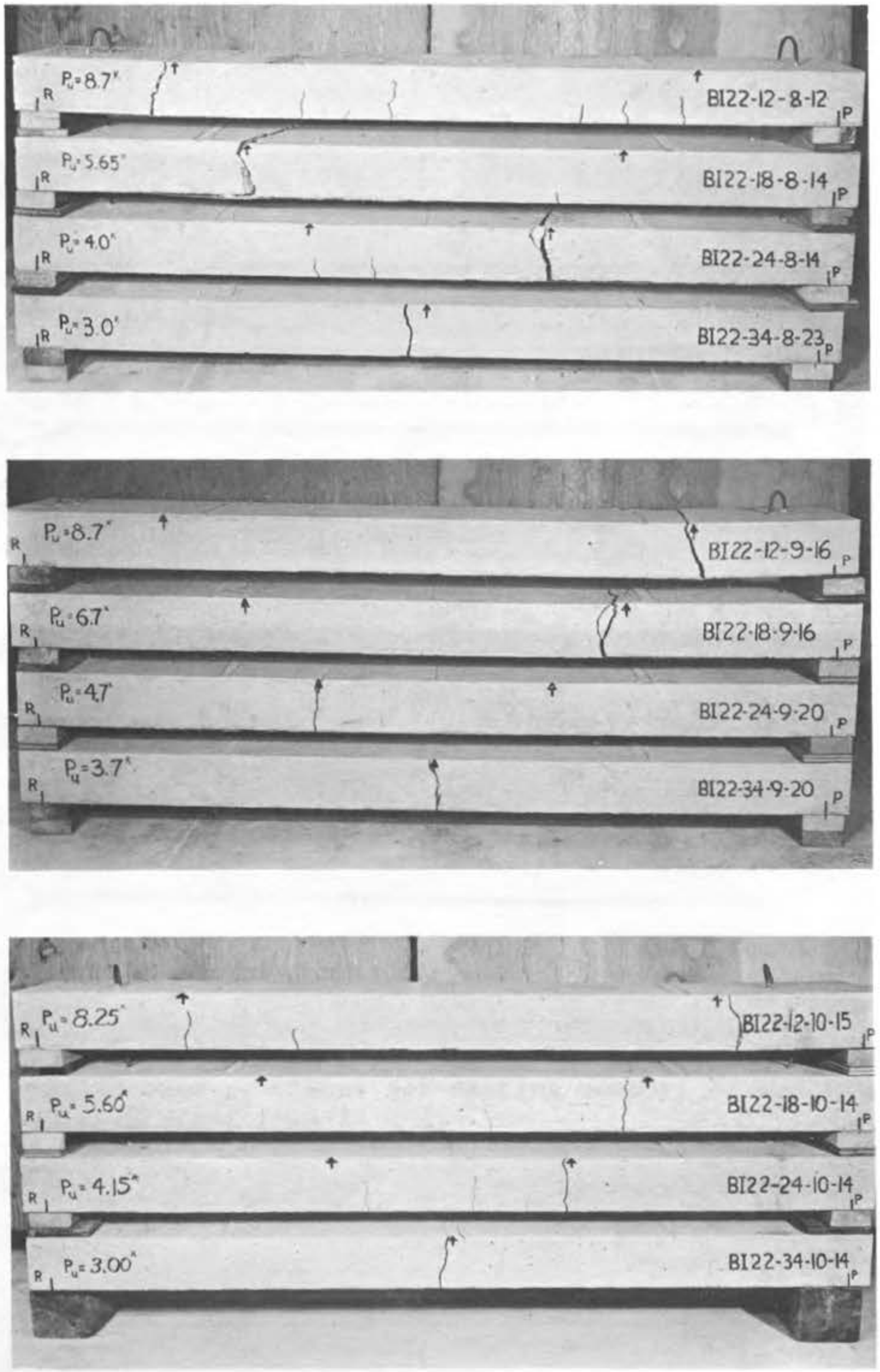

Fig. 9. Failed beam specimens for casting numbers 8, 9, and 10 using 22-gage steel form I.

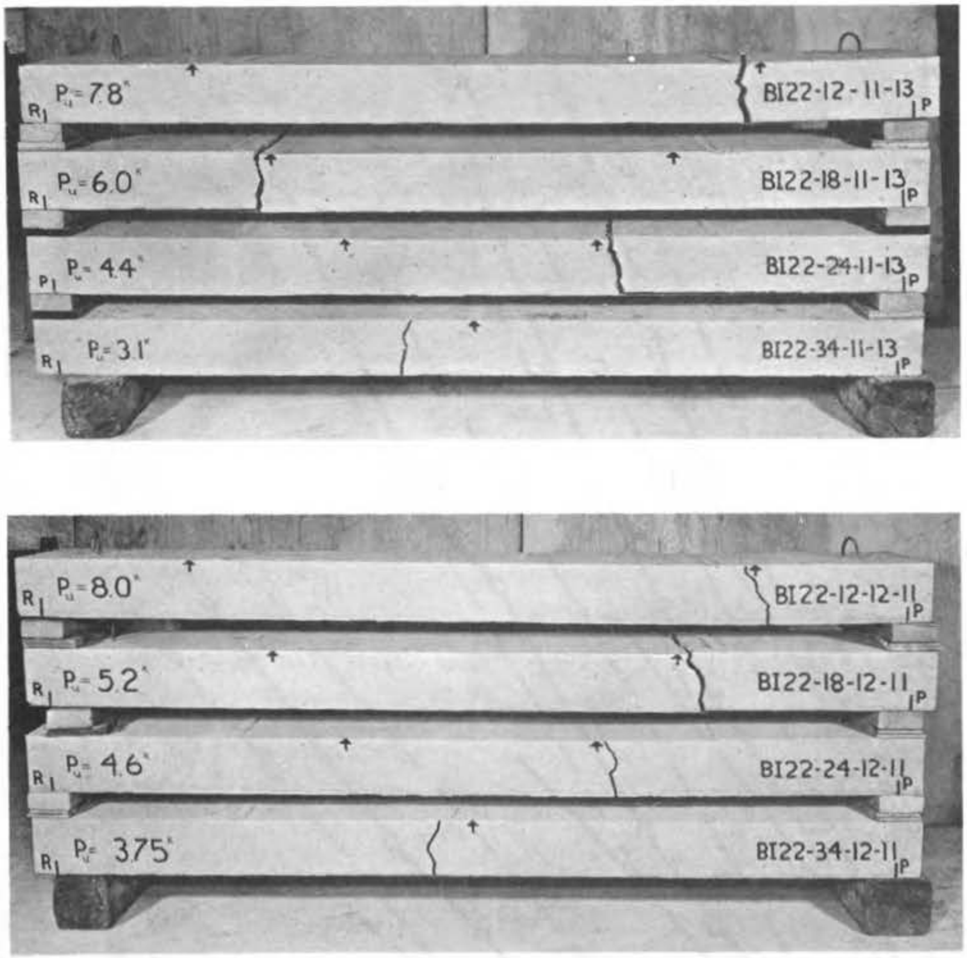

Fig. 10. Failed beam specimens for casting numbers 11 and 12 using 22-gage steel form I.

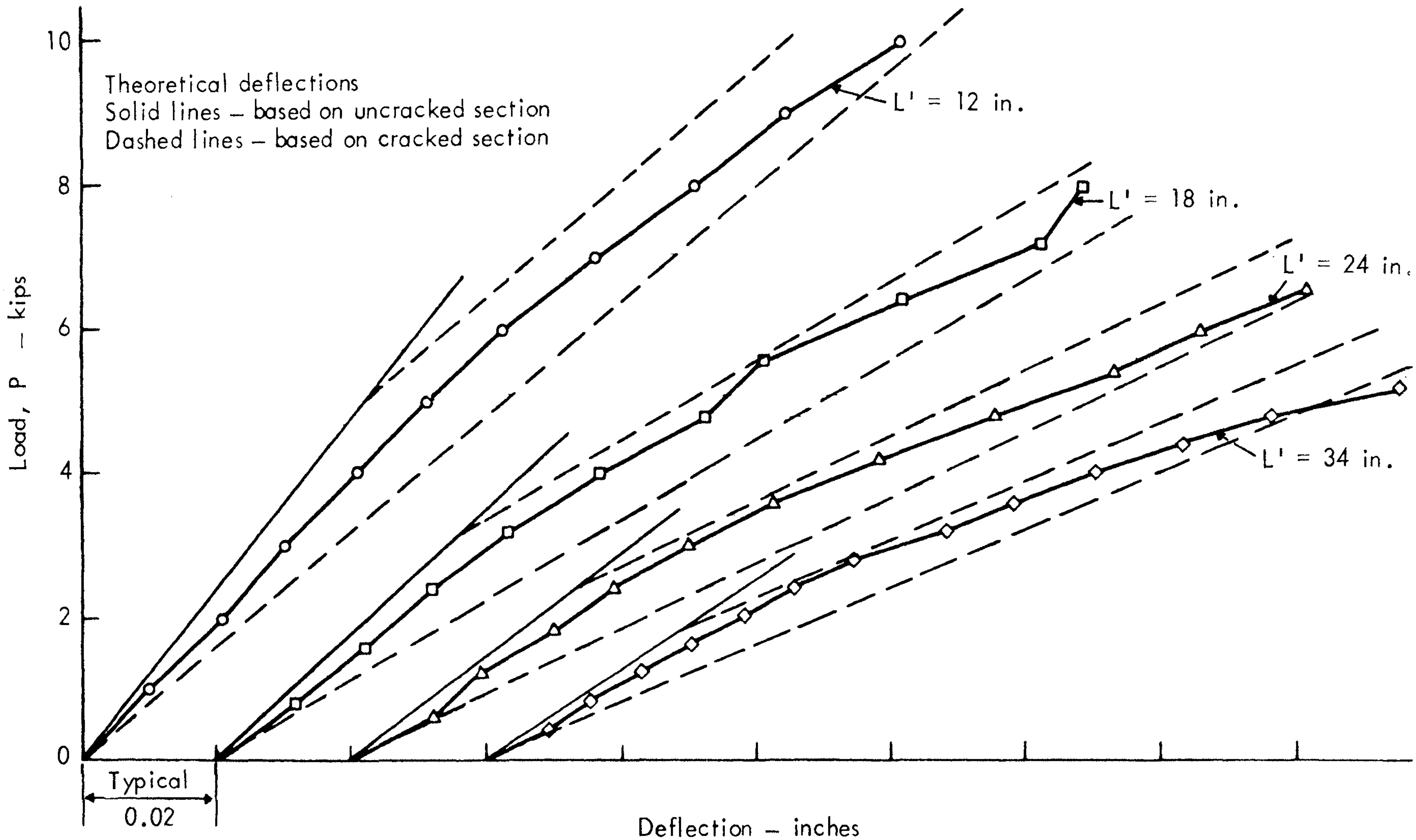

Fig. 11. Applied load, P , vs deflection for embedment lengths of 12, 18, 24, and 34 in. (each curve is the average of 5 tests) for beams consisting of 18-gage steel form I.

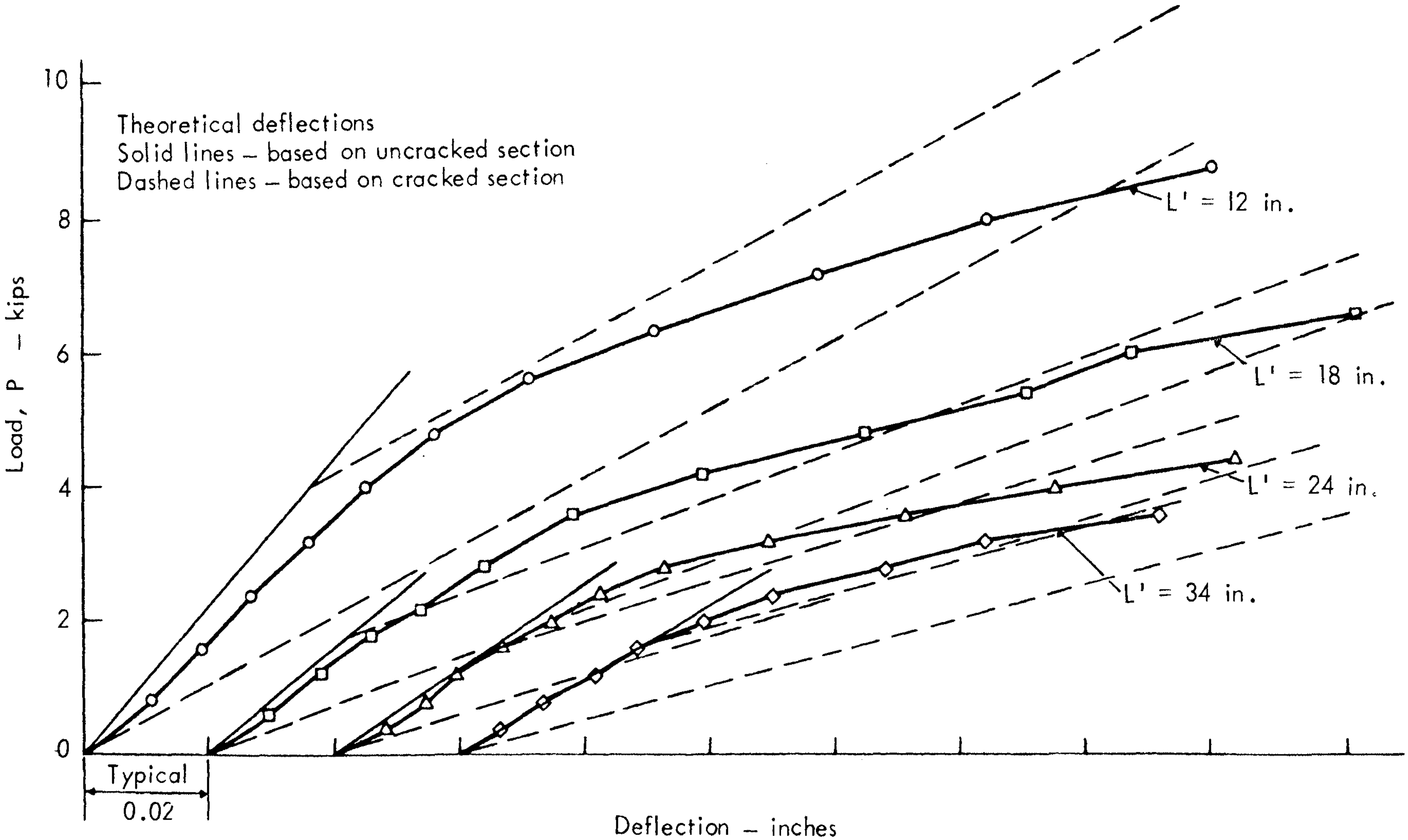

Fig. 12. Applied load, P , vs deflection for embedment length of 12, 18, 24, and 34 in. (each curve is the average of 5 tests) for beams consisting of 22-gage steel form I

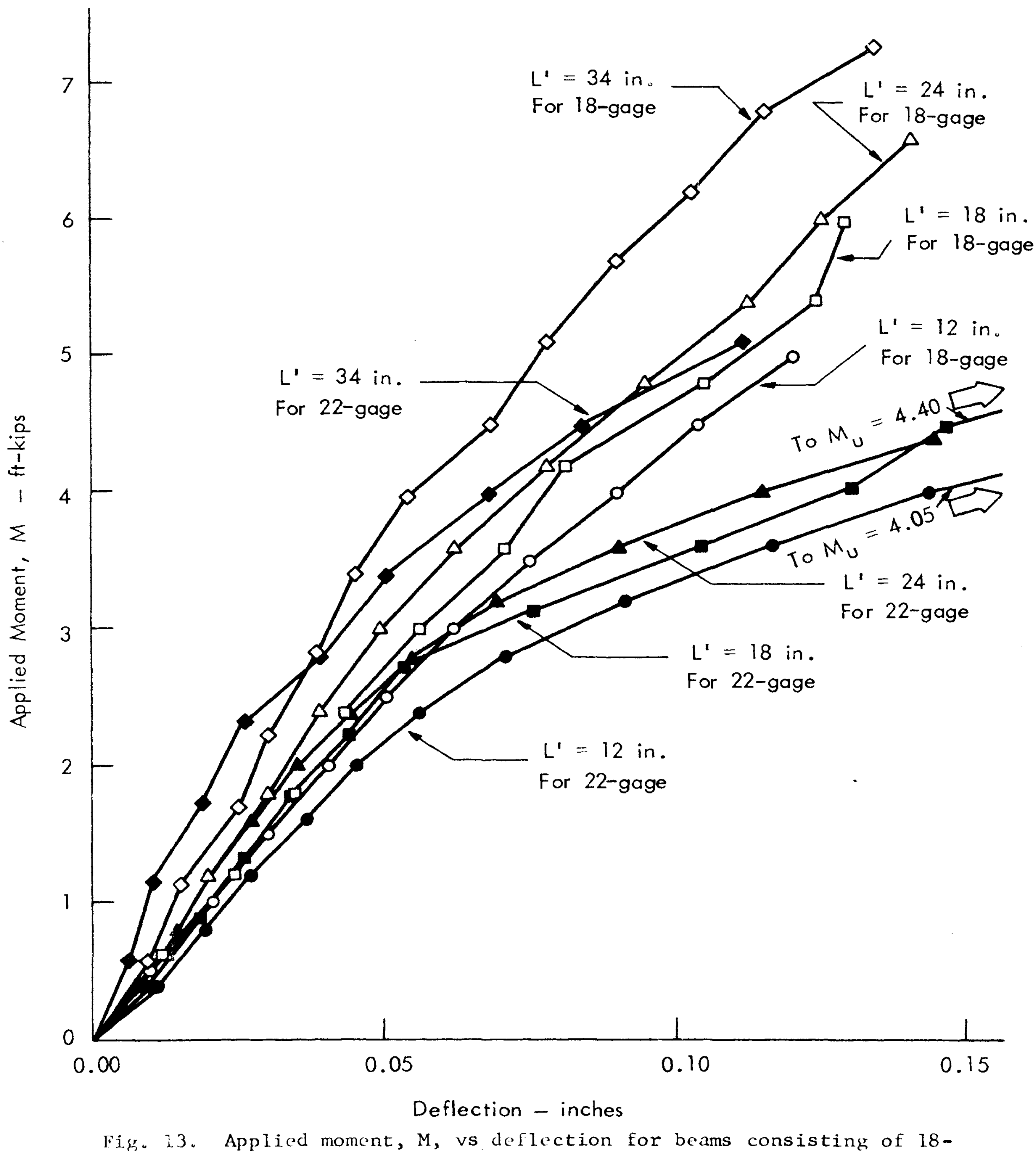

Fig. 13. Applied moment, M, vs deflection for beams consisting of 18- and 22-gage steel form I.

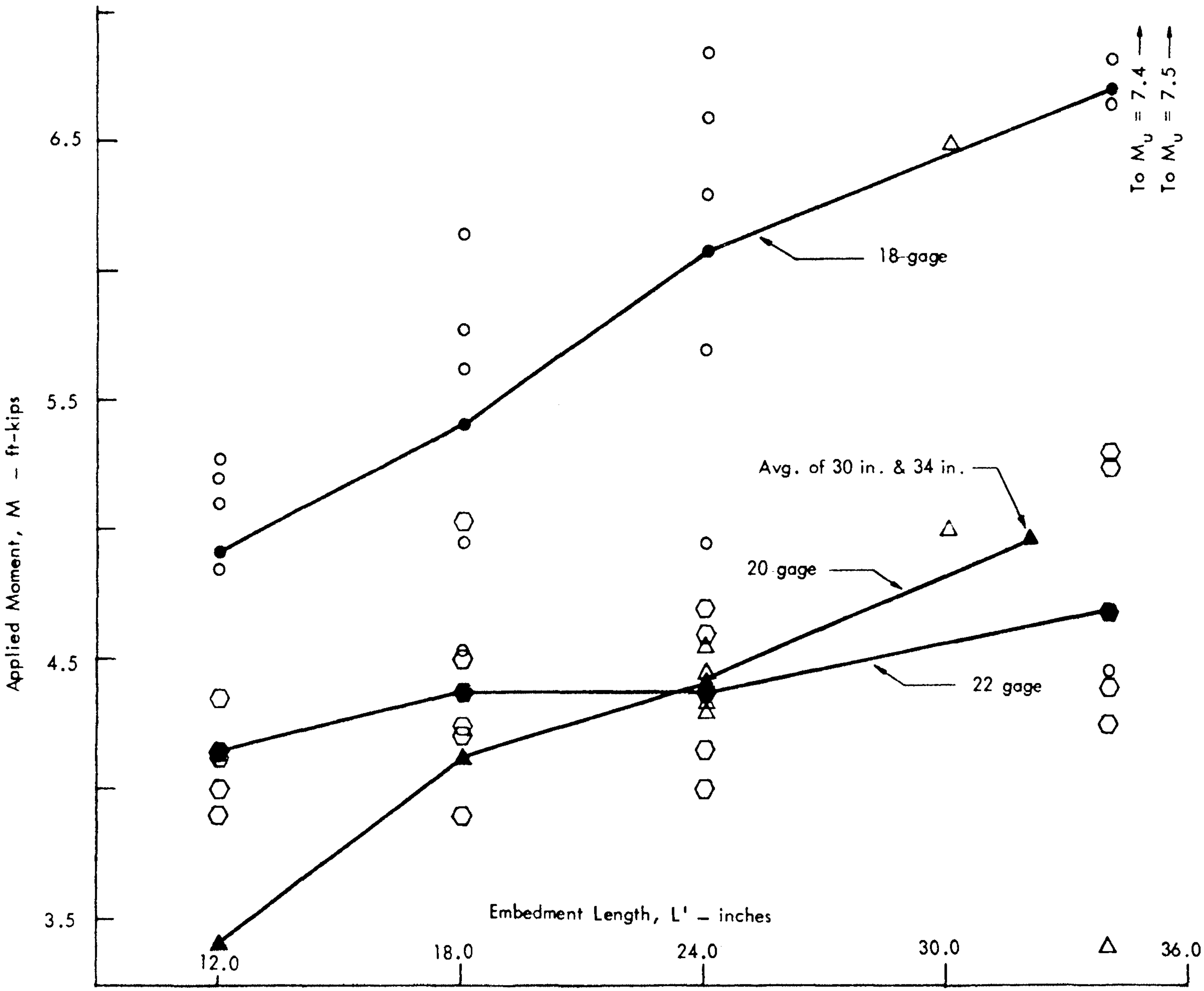

Fig. 14. Applied moment, M , vs embedment length, L', for beams consisting of 18- and 22-gage steel form I.

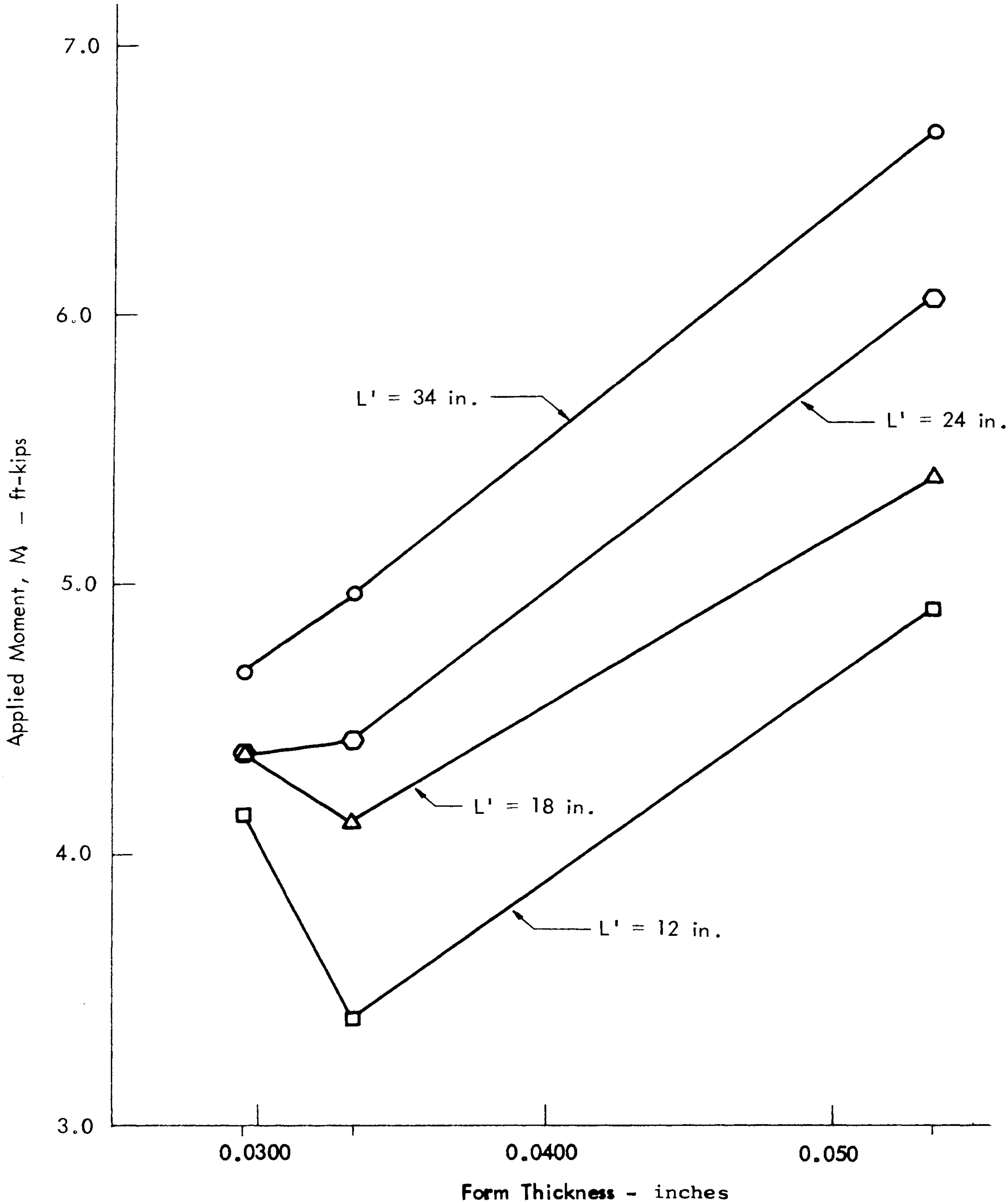

Fig. 15. Applied moment, M, vs form thickness for embedment lengths of 12, 18, 24, and 34 in. for form I.

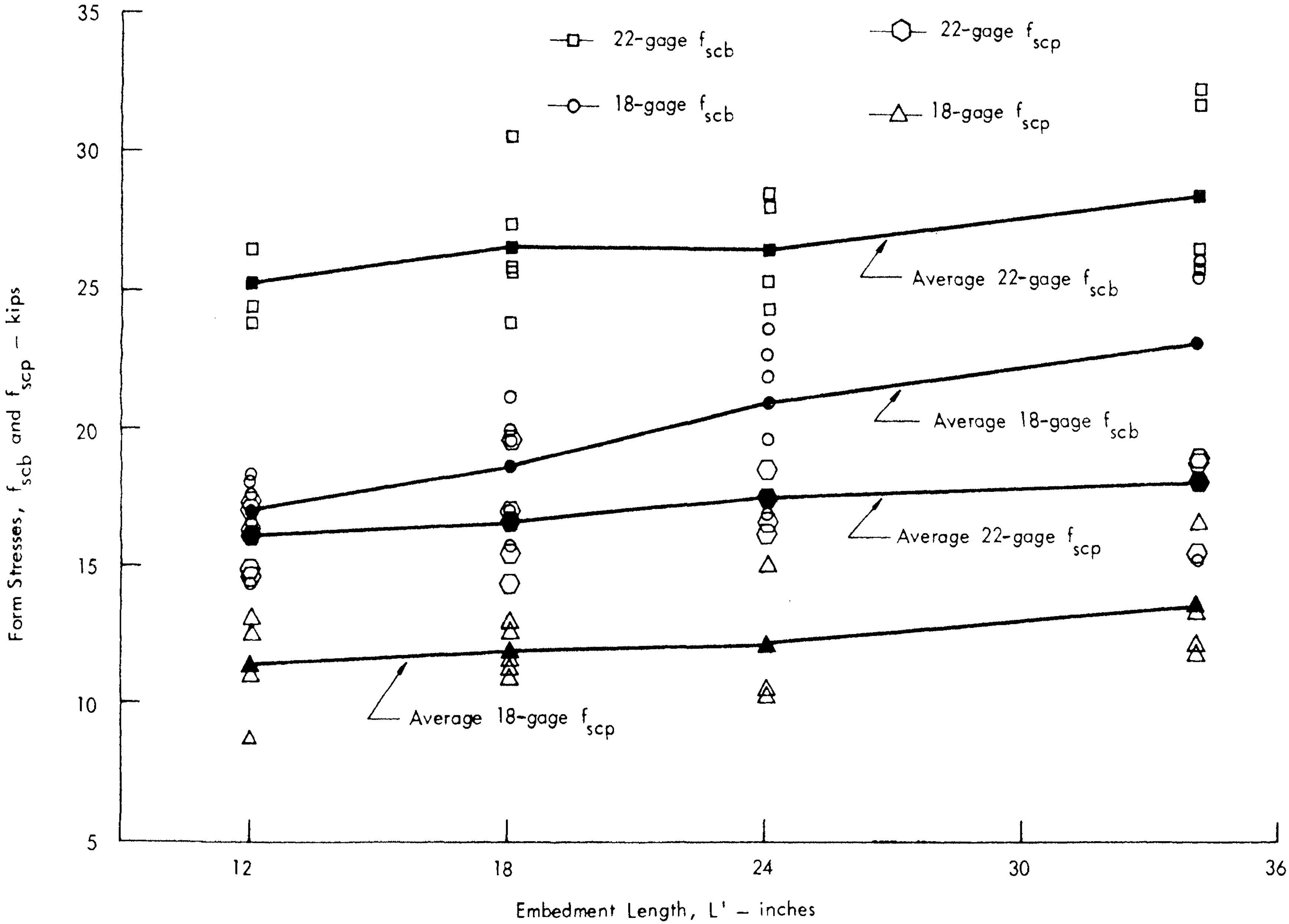

Fig. 16. Form stresses, f_{scp} and f_{scb}, vs embedment length, L', for beams consisting of 18- and 22-gage steel form I.

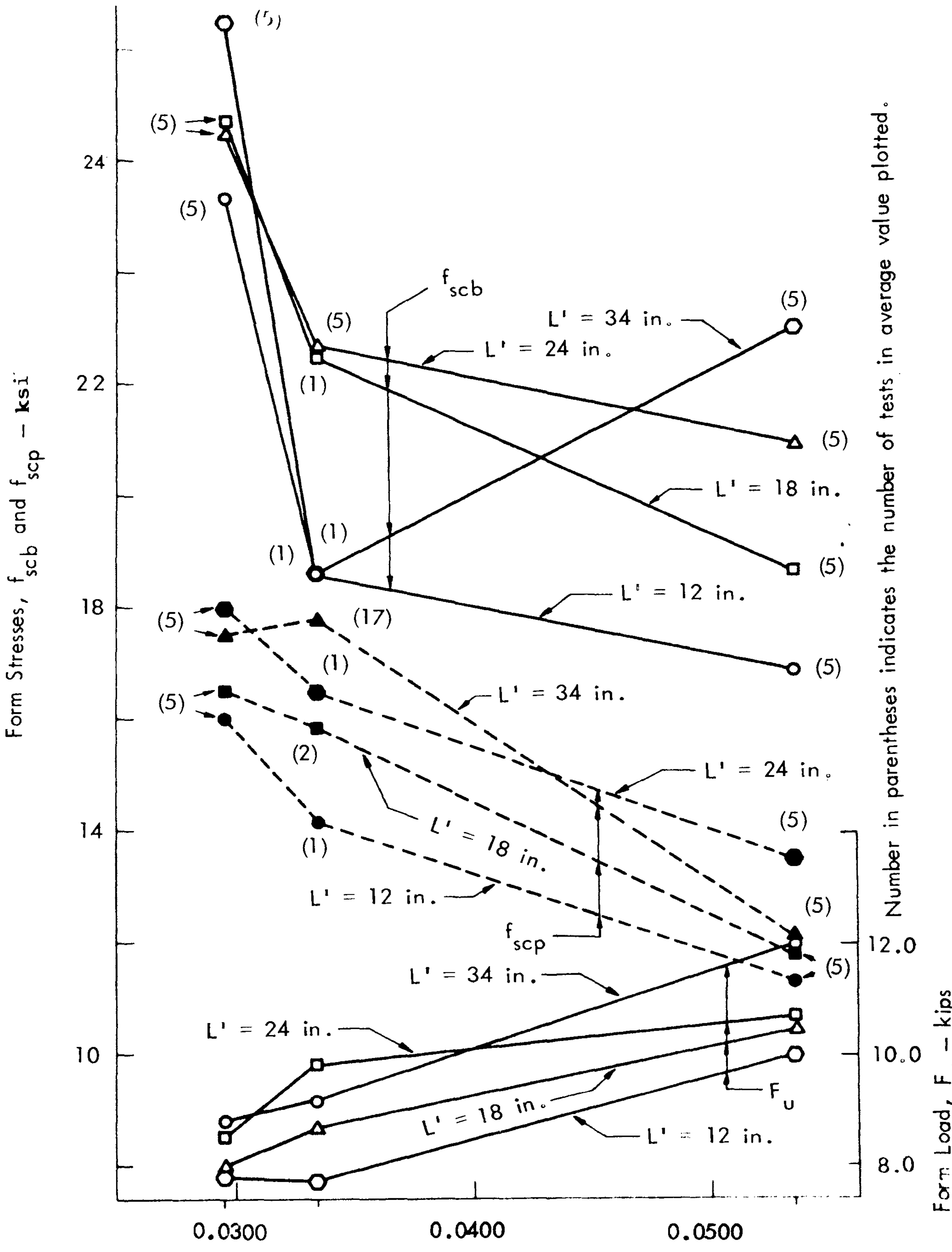

Fig. 17. Form stresses, f_{scp} and f_{scb}, and form load, F_u, vs form thickness for embedment lengths, L', of 12, 18, 24, and 34 in. for form I.

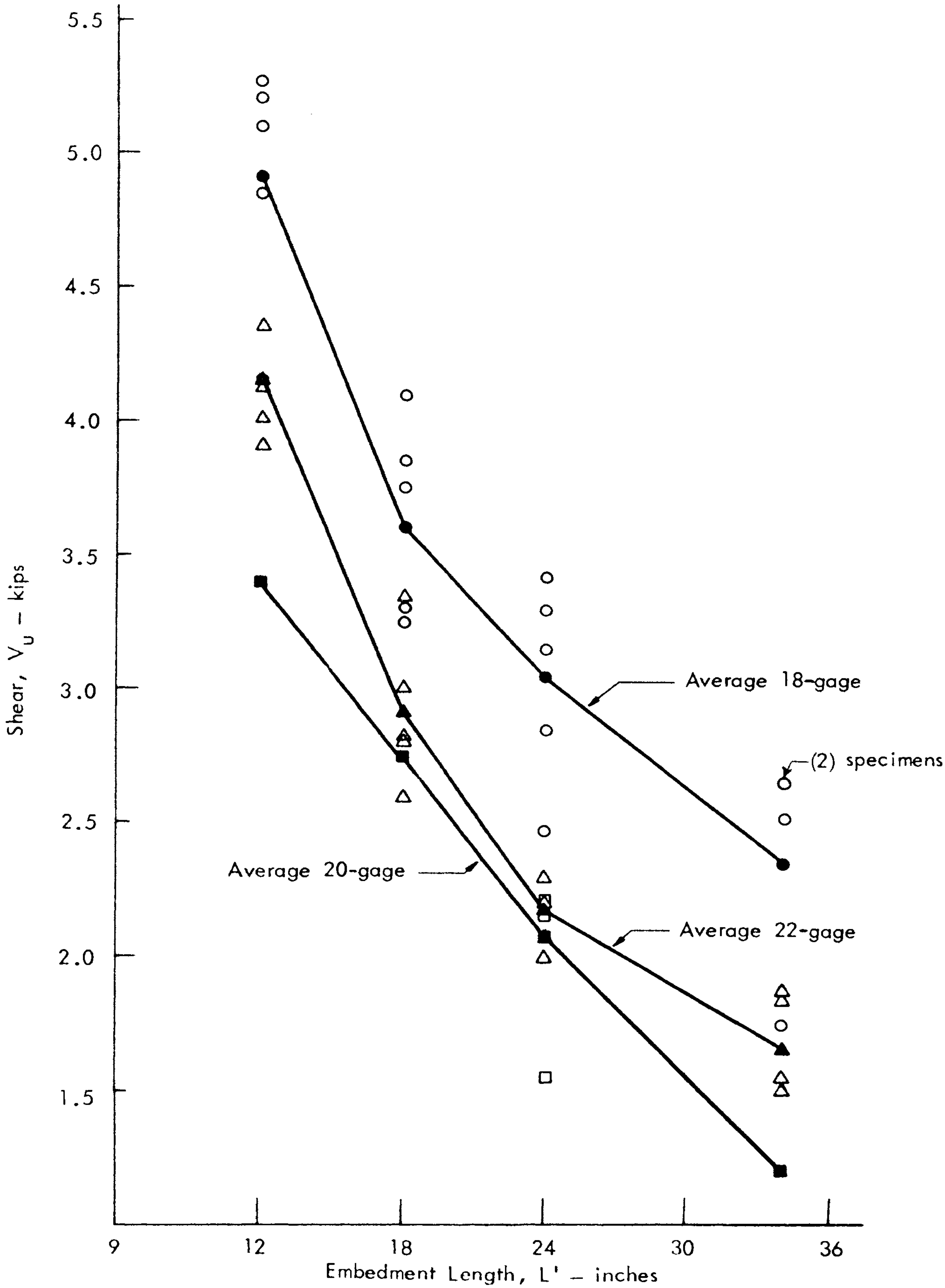

Fig. 18. Shear, V_u, vs embedment length, L', for beams consisting of 18- and 22-gage steel form I.

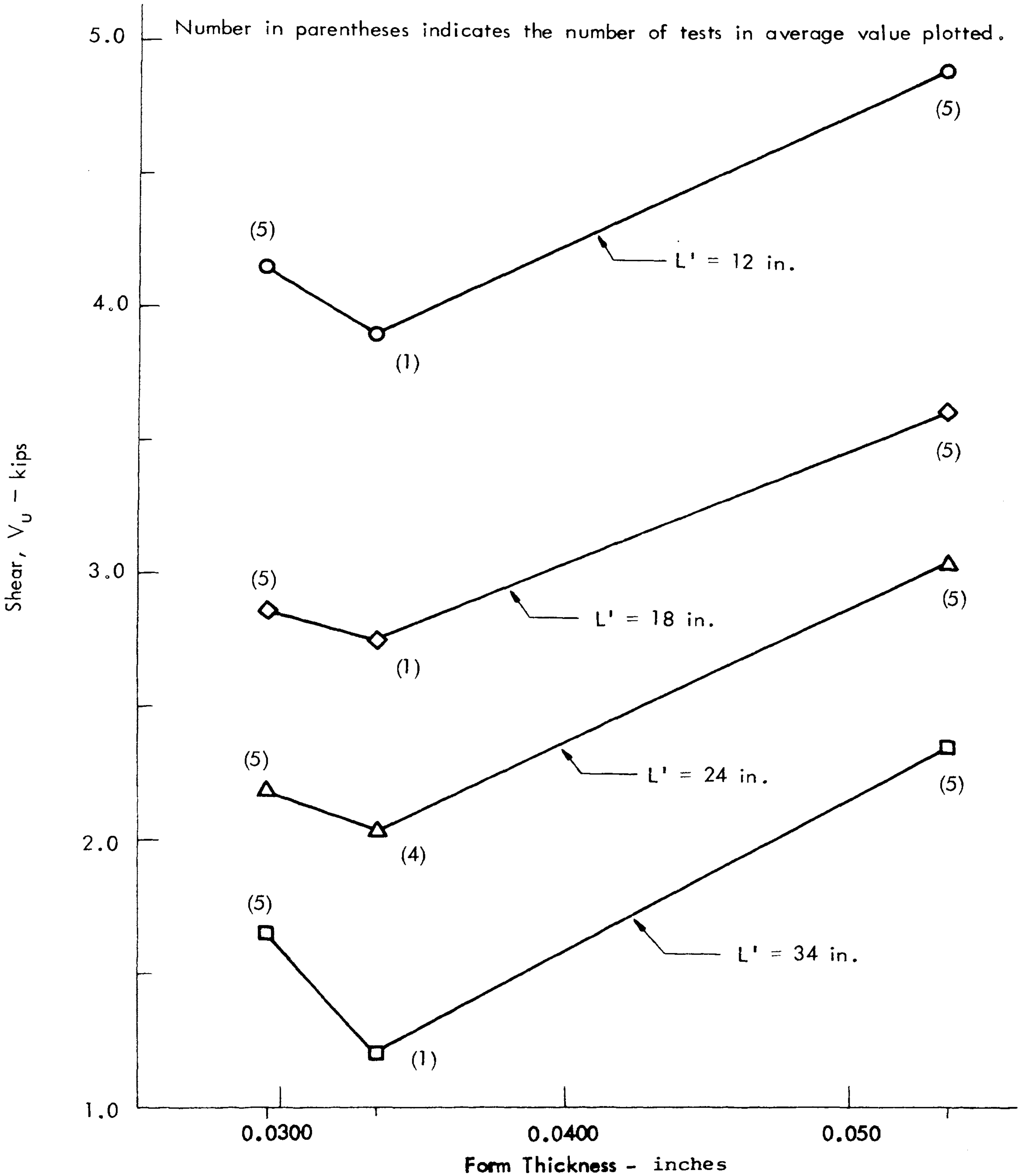

Fig. 19. Shear, V_u, vs form thickness for embedment length, L', of 12, 18, 24, and 34 in. for form I.

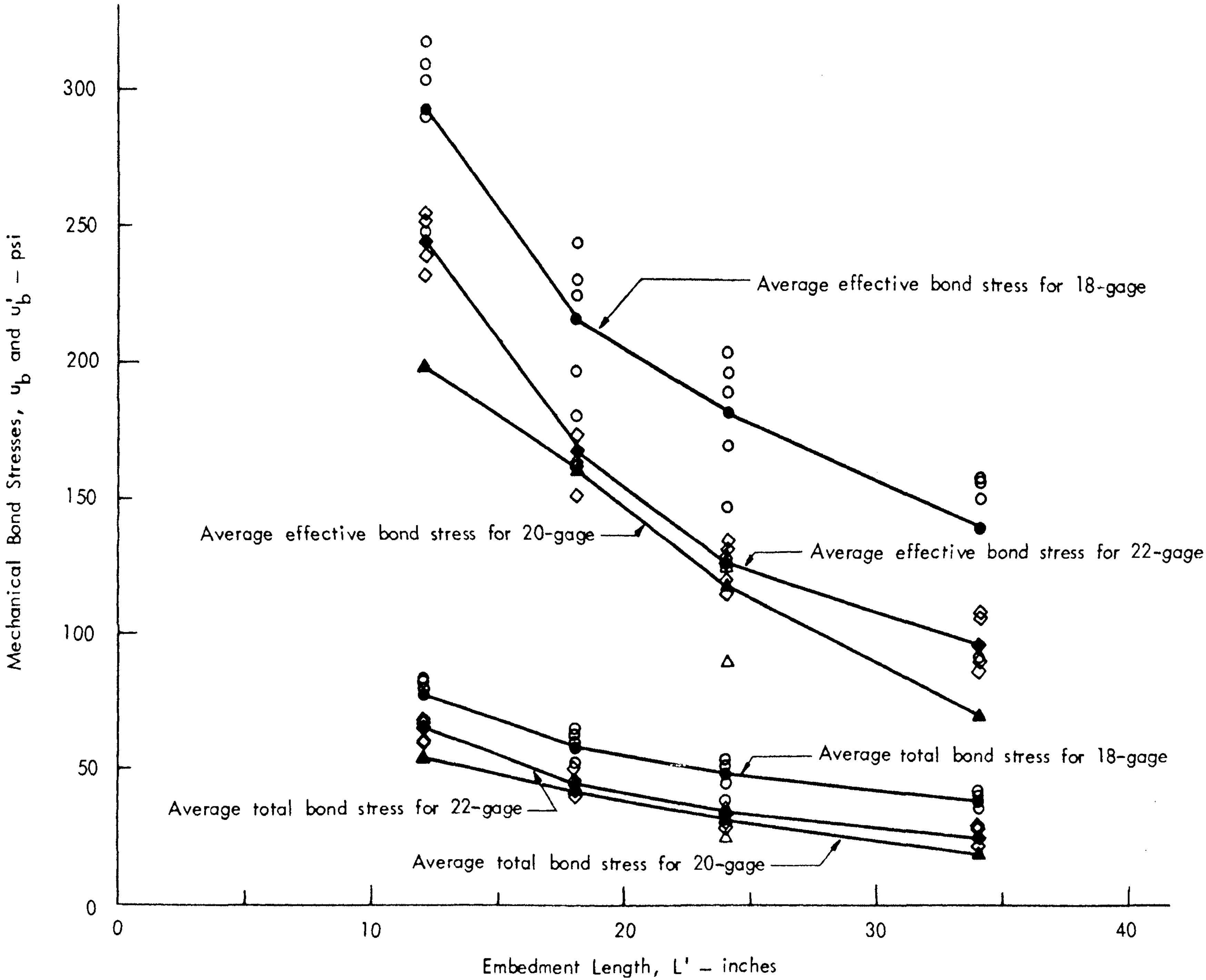

Fig. 20. Mechanical bond stresses, u_b and u'_b, vs embedment length, L', for beams consisting of 18- and 22-gage steel form I.

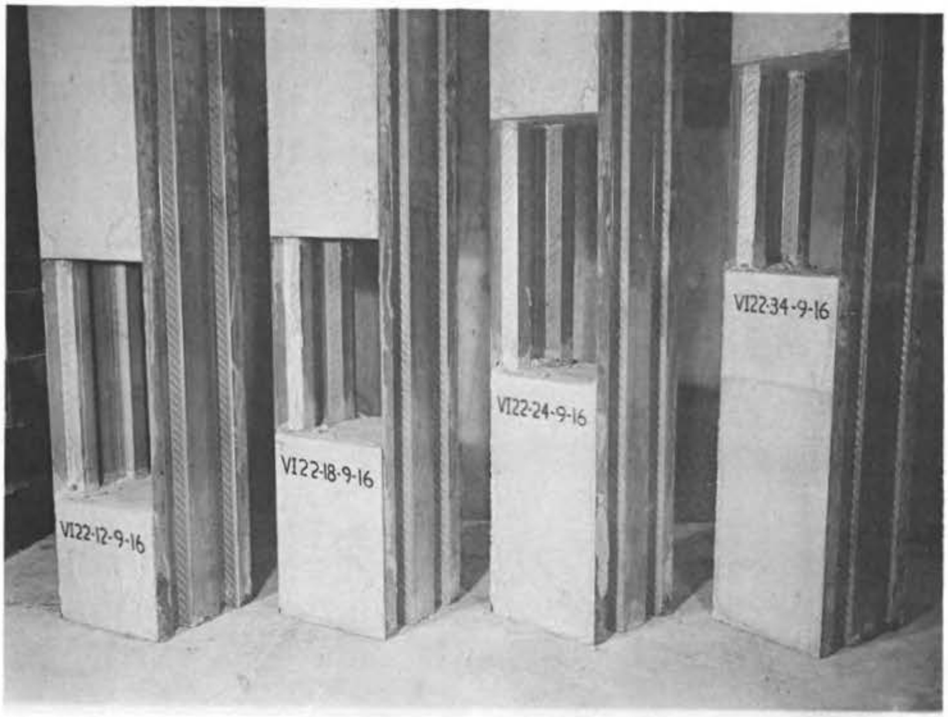

Fig. 21. Typical embedment lengths for pushout specimens.

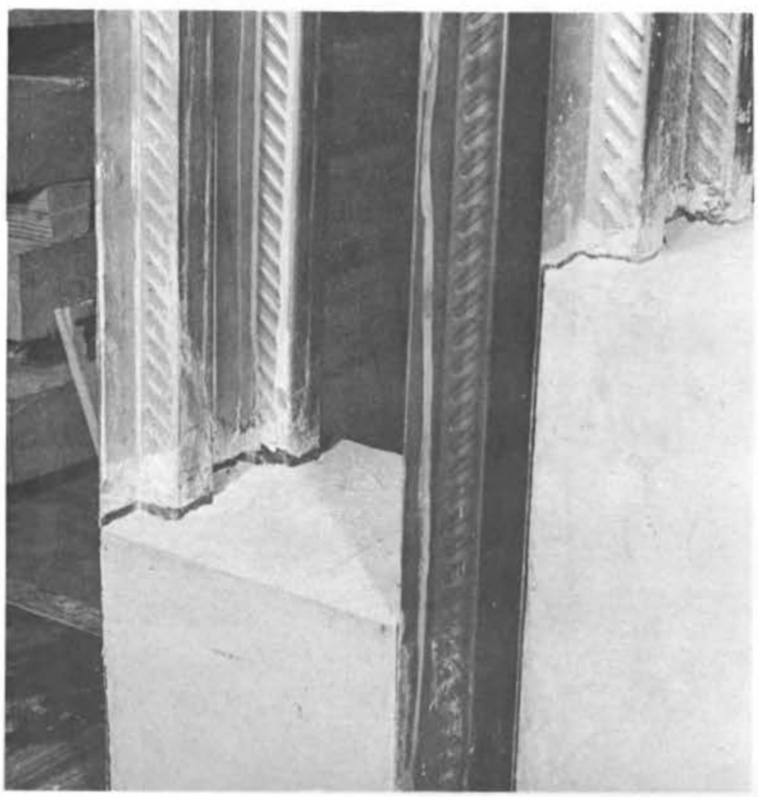

Fig. 22. Typical vertical pushout failure for form I.

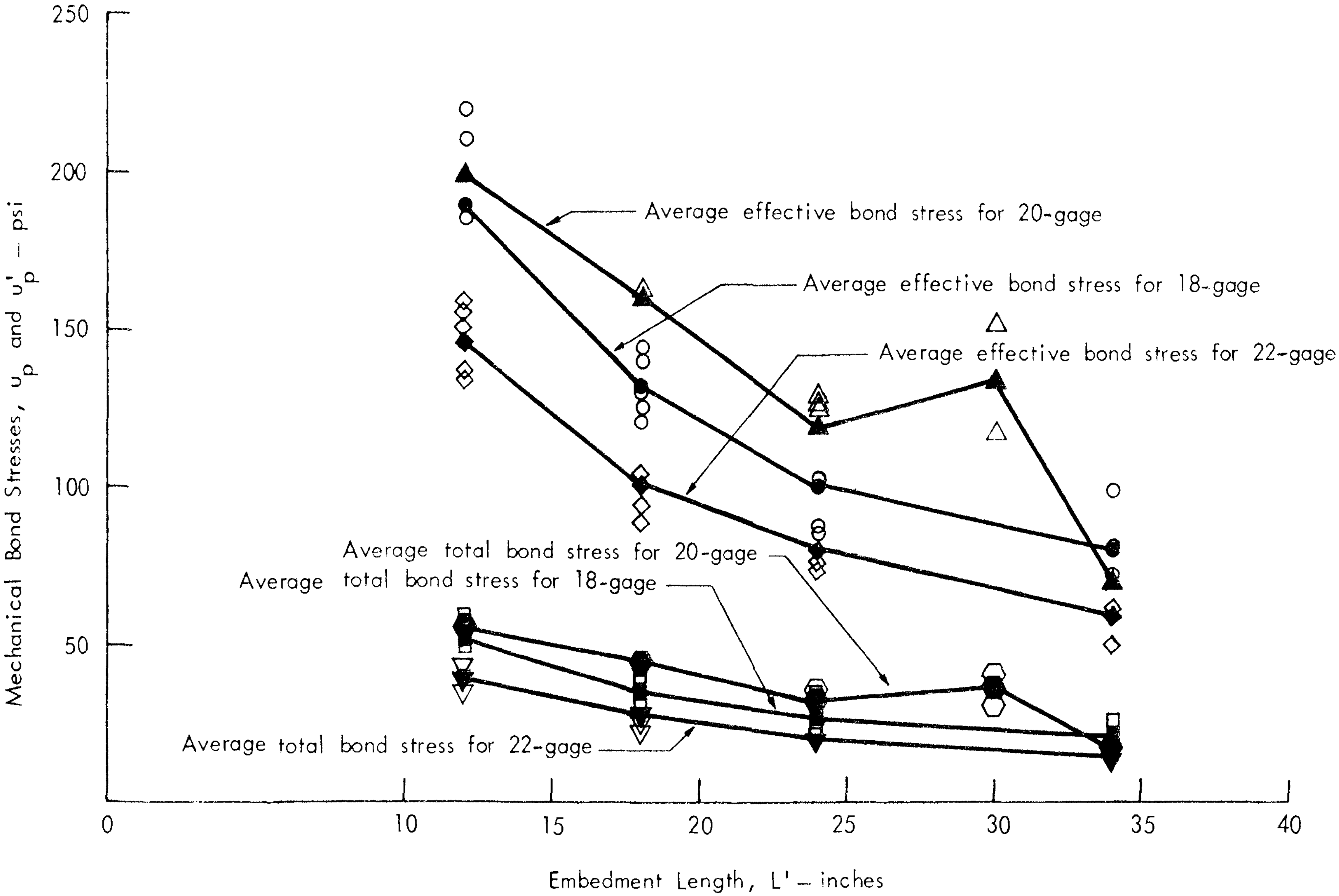

Fig. 23. Mechanical bond stresses, u_p and u'_p, vs embedment length, L', for beams consisting of 18- and 22-gage steel form I.

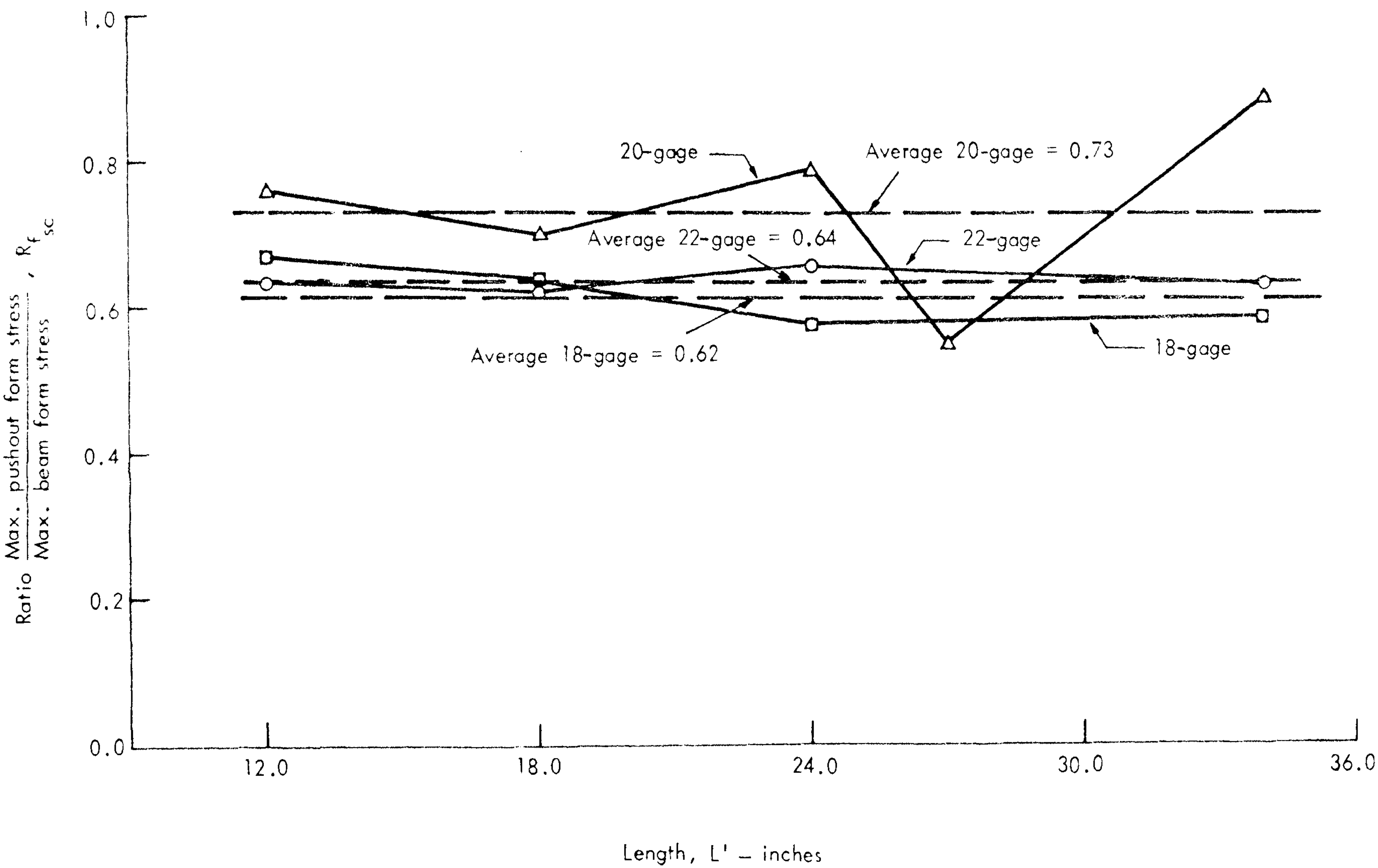

Fig. 25. Ratio, $R_{f_{sc}}$, vs embedment length, L', for specimens consisting of 18- and 22-gage steel form I.

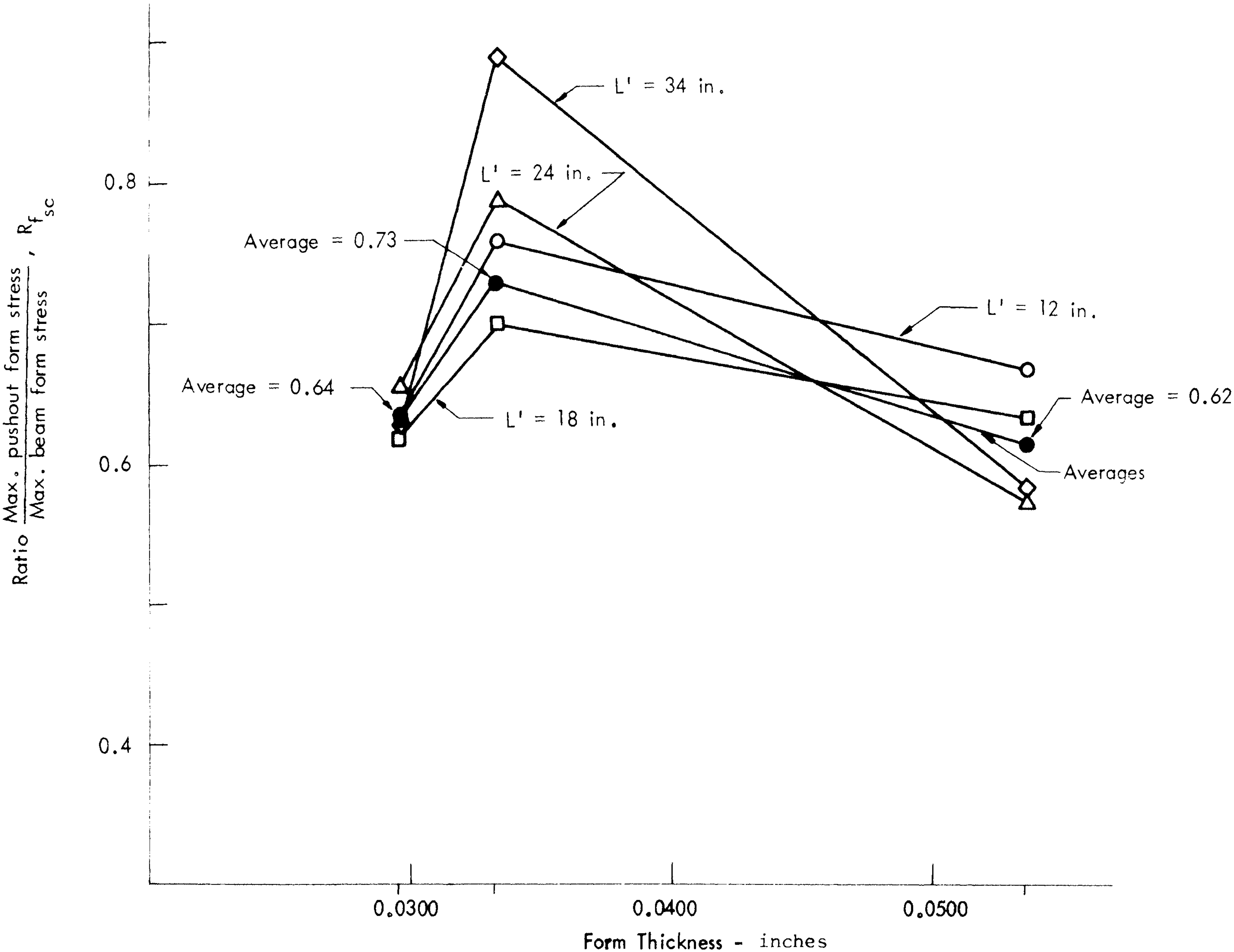

Fig. 26. Ratio, $R_{f_{sc}}$, vs form thickness for embedment lengths of 12, 18, 24 and 34 in. for form I.

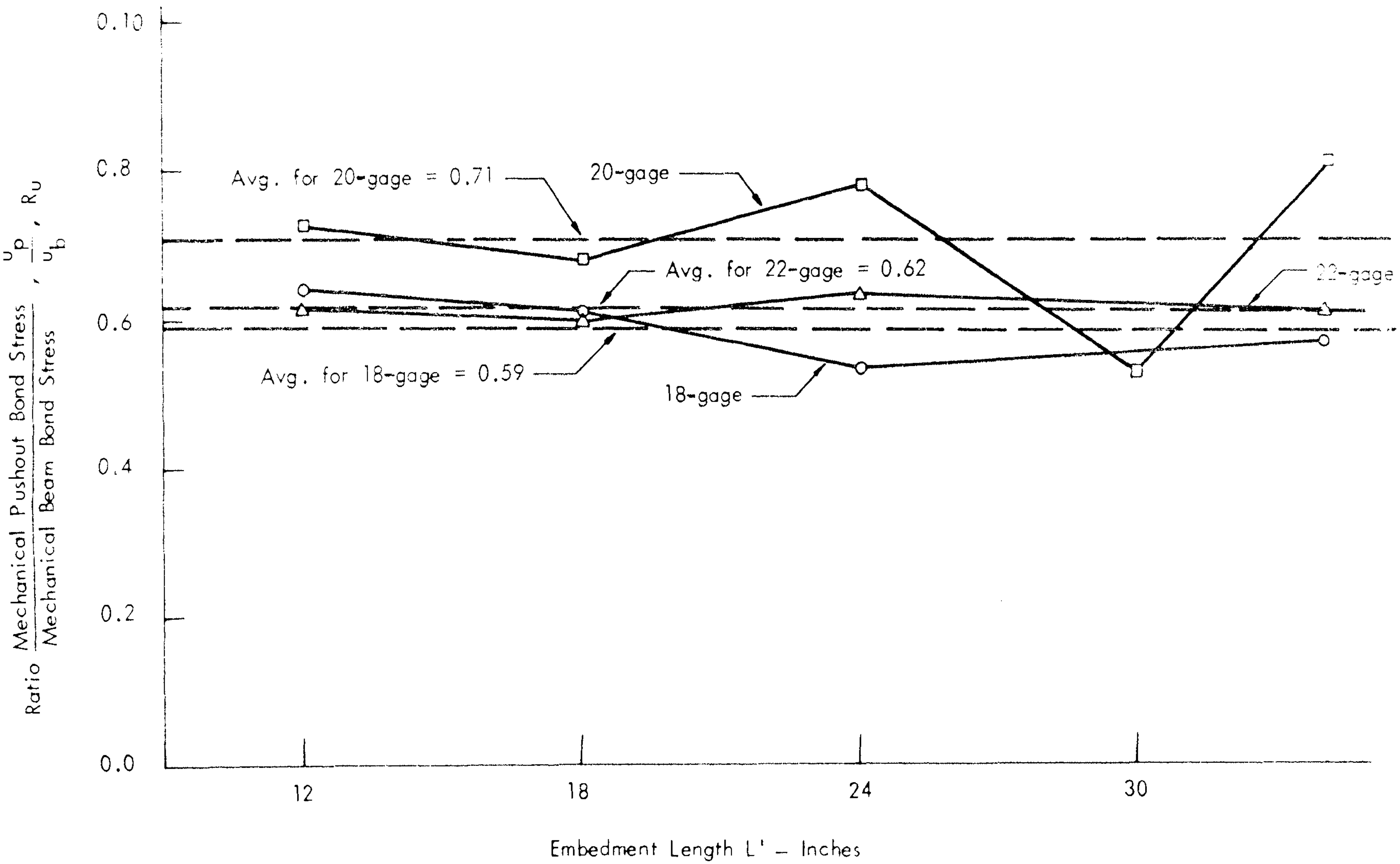

Fig. 27. Ratio, R_u, vs embedment length, L', for specimens of 18- and 22-gage steel form I.

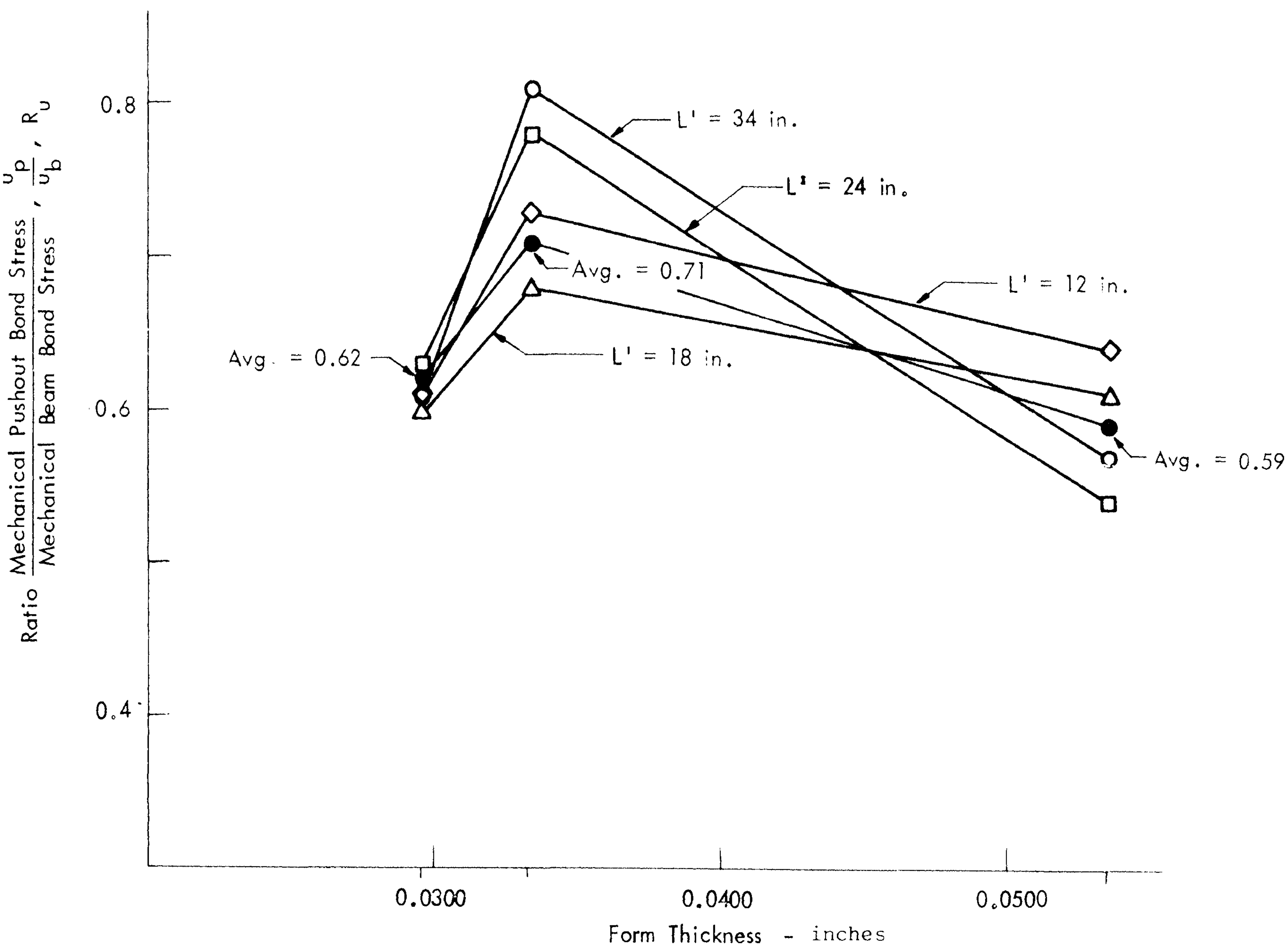

Fig. 28. Ratio, R_u, vs form thickness for embedment lengths of 12, 18, 24, and 34 in. for form I.

APPENDIX C. TABLES

Table 1. Typical properties of form I.

Property	18-gage	20-gage[(a)]	22-gage
Width, b — in.	12	12	12
Steel area, A_s — $in.^2$	0.884	0.545	0.487
Steel centroid, $\overline{y}$ — in.	0.630	0.620	0.618
Moment of inertia, I_s — $in.^4$	0.342	0.211	0.189
Steel thickness, t — in.	0.0535	0.033	0.0295
Total perimeter, Σ_o — in.	16.52	16.52	16.52
Embossment perimeter, Σ_o' — in. (effective)	4.40	4.40	4.40
Depth of form, d_s — in.	1.55	1.55	1.55
Modulus of elasticity, E_s — psi $\times 10^6$	29.3	29.1	28.7
Proportional limit — psi	29,700	32,500	28,300
Yield strength (0.1% offset) — psi	40,200	40,050	39,800
Rupture strength — psi	44,900	48,850	48,900
Yield point — psi	41,200	40,150	40,000
Ultimate strength — psi	52,300	55,300	54,200
Percent elongation in 8 in.	22.9	24.1	19.3
Percent elongation in 2 in.	36.8	34.5	31.8

[(a)] The data for the 20-gage steel was taken from the August report, Tables 2a and 2b.

Table 2. Summary of concrete properties used in casting specimens. (See Table 3 in August report.)

Casting number	Date of casting	Cement properties[c] sacks/yd	Aggregate properties: Fine (lb/yd)	Aggregate properties: Coarse (lb/yd)	Aggregate properties: Max size (in.)	Water added[b] (gal/yd)	Slump[a] (in.)	Compressive strength − f'_c (psi)	Age of f'_c (days)	Modulus of elasticity[d] (psi × 10^6)	w (lb/ft^3)
8	9/28/68	5	1467	1870	3/4	28	3 1/2	3849	12	3.57	145
8	9/28/68	5	1467	1870	3/4	28	3 1/2	4606	23	3.91	145
9	10/8/68	5	1466	1868	3/4	24	3	4432	14	3.80	144
9	10/8/68	5	1466	1868	3/4	24	3	4720	20	3.92	144
10	11/5/68	5	1466	1869	3/4	27	3 1/2	3350	11	3.30	144
10	11/5/68	5	1466	1869	3/4	27	3 1/2	3577	14	3.41	144
11	11/14/68	5	1466	1868	3/4	22	3 1/2	3426	11	3.37	145
11	11/14/68	5	1466	1868	3/4	22	3 1/2	3634	13	3.47	145
12	11/22/68	5	1486	1868	3/4	26	4	3573	11	3.41	144

[a] No admixtures were added to any concrete castings.

[b] Water added includes only that added at plant plus water added on truck.

[c] Cement used for all concrete castings was Type 1 of Northwestern brand.

[d] Values computed in accordance with ACI empirical formula.

Table 3. Computed quantities needed to obtain M_{ab}, M_{ac}, and M_c in Table 5.

Casting number	w (lb/ft^3)	f'_c (psi)	E_c (psi × 10^6)	E_s (psi × 10^6)	n	2n	kd — in. 18-gage	kd — in. 22-gage	$f_c = 0.45\ f'_c$ (psi)
8	145	3849	3.57	29.0	8.12	16.24	1.765	1.401	1732
8	145	4606	3.91	29.0	7.42	14.84	1.706	1.350	2072
9	144	4432	3.80	29.0	7.63	15.26	1.724	1.366	1994
9	144	4720	3.92	29.0	7.40	14.80	1.704	1.348	2124
10	144	3350	3.30	29.0	8.79	17.58	1.817	1.446	1508
10	144	3577	3.41	29.0	8.50	17.00	1.795	1.426	1610
11	145	3426	3.37	29.0	8.61	17.22	1.803	1.434	1542
11	145	3634	3.47	29.0	8.36	16.72	1.784	1.417	1635
12	144	3573	3.41	29.0	8.50	17.00	1.795	1.426	1608

Steel gage	Casting number	f'_c (psi)	nA_s	nI_s	I_T	I_T/n	4d (in.)	A_s (in.^{2})
18	8	3849	7.178	2.777	73.480	9.049	17.48	0.884
18	8	4606	6.559	2.537	69.366	9.349	17.48	0.884
18	9	4432	6.744	2.609	70.322	9.217	17.48	0.884
18	9	4720	6.541	2.530	68.811	9.299	17.48	0.884
18	10	3350	7.770	3.006	77.644	8.833	17.48	0.884
18	10	3577	7.514	2.907	75.863	8.925	17.48	0.884
18	11	3426	7.611	2.944	76.541	8.890	17.48	0.884
18	11	3634	7.390	2.859	74.989	8.970	17.48	0.884
18	12	3573	7.514	2.907	75.863	8.925	17.48	0.884
22	8	3849	3.954	1.534	47.700	5.874	17.528	0.487
22	8	4606	3.613	1.402	44.458	5.992	17.528	0.487
22	9	4432	3.715	1.442	45.430	5.954	17.528	0.487
22	9	4720	3.603	1.398	44.362	5.995	17.528	0.487
22	10	3350	4.280	1.661	50.648	5.762	17.528	0.487
22	10	3577	4.139	1.606	49.371	5.808	17.528	0.487
22	11	3426	4.193	1.627	49.862	5.791	17.528	0.487
22	11	3634	4.071	1.580	48.750	5.831	17.528	0.487
22	12	3573	4.139	1.606	49.371	5.808	17.528	0.487

Table 4. Computed quantities needed to obtain M'_u in Table 5.

Steel gage	Casting number	A_s (in.^{2})	f_y (psi)	d (in.)	C_{scb} (in.)	C_{sb} (in.)	f'_c (psi)	a (in.)	a/2 (in.)	M'_u (ft/lb)
18	8	0.884	40,600	4.370	2.605	3.235	3849	0.914	0.457	11,703
18	8	0.884	40,600	4.370	2.664	3.294	4606	0.764	0.382	11,928
18	9	0.884	40,600	4.370	2.646	3.276	4432	0.764	0.382	11,928
18	9	0.884	40,600	4.370	2.666	3.294	4720	0.745	0.372	11,957
18	10	0.884	40,600	4.370	2.553	3.183	3350	1.050	0.525	11,500
18	10	0.884	40,600	4.370	2.575	3.205	3577	0.984	0.492	11,598
18	11	0.884	40,600	4.370	2.567	3.197	3426	1.027	0.514	11,533
18	11	0.884	40,600	4.370	2.586	3.216	3634	0.968	0.484	11,622
18	12	0.884	40,600	4.370	2.575	3.205	3573	0.985	0.492	11,598
22	8	0.487	40,600	4.382	2.981	3.382	3849	0.504	0.252	6,805
22	8	0.487	40,600	4.382	3.032	3.650	4606	0.421	0.210	6,874
22	9	0.487	40,600	4.382	3.016	3.634	4432	0.437	0.218	6,861
22	9	0.487	40,600	4.382	3.034	3.652	4720	0.411	0.206	6,881
22	10	0.487	40,600	4.382	2.936	3.544	3350	0.579	0.289	6,743
22	10	0.487	40,600	4.382	2.956	3.574	3577	0.541	0.271	6,774
22	11	0.487	40,600	4.382	2.948	3.566	3426	0.566	0.283	6,754
22	11	0.487	40,600	4.382	2.965	3.583	3634	0.533	0.267	6,780
22	12	0.487	40,600	4.382	2.956	3.574	3573	0.542	0.271	6,774

Table 5. Tabulation of design and ultimate moments. (See Table 1 in August report.)

Steel gage	Casting number	f'_c (psi)	Compressive depth — kd (in.)	Manufacturer's design moment for steel stress of 20,000 psi		Ultimate moment by ACI code, M'_u (ft-lb)	Allowable moment, for $f_c = 0.45\ f'_c$, M_c (ft-lb)
				M_{ac}[a] (ft-lb)	M_{ab}[b] (ft-lb)		
18	8	3,849	1.765	5,789	4,662	11,703	6,009
18	8	4,606	1.706	5,849	4,730	11,928	7,021
18	9	4,432	1.724	5,806	4,689	11,928	6,778
18	9	4,720	1.704	5,813	4,702	11,957	7,148
18	10	3,350	1.817	5,766	4,625	11,500	5,370
18	10	3,577	1.795	5,777	4,641	11,598	5,670
18	11	3,426	1.803	5,772	4,635	11,533	5,455
18	11	3,634	1.784	5,781	4,649	11,622	5,727
18	12	3,573	1.795	5,777	4,641	11,598	5,663
22	8	3,849	1.401	3,284	2,720	6,805	4,914
22	8	4,606	1.350	3,294	2,736	6,874	5,686
22	9	4,432	1.366	3,290	2,731	6,861	5,526
22	9	4,720	1.348	3,293	2,736	6,881	5,825
22	10	3,350	1.446	3,271	2,702	6,743	4,401
22	10	3,577	1.426	3,275	2,708	6,774	4,645
22	11	3,426	1.434	3,274	2,707	6,754	4,468
22	11	3,634	1.417	3,278	2,712	6,780	4,688
22	12	3,573	1.426	3,275	2,708	6,774	4,639

[a] Based on $M_{ac} = f_s I_T / 12\ nc_{scb}$.

[b] Based on $M_{ab} = f_s I_T / 12\ nc_{sb}$.

Table 6. Experimental test results for beams using 18- and 22-gage steel form I. (See Table 12 in August report.)

Specimen designation	Ultimate beam load, P_u (lb)	Ultimate shear V_u (lb)	Ultimate moment M_u (ft-lb)	Form stress – psi: Centroidal f_{scb}	Form stress – psi: Bottom f_{sb}
<u>18-gage</u>					
BI18-12-8-23	9,700	4,850	4,850	16,585	20,510
BI18-12-9-14	10,200	5,100	5,100	17,570	21,750
BI18-12-10-11	10,550	5,275	5,275	18,300	22,810
BI18-12-11-13	8,300	4,150	4,150	14,360	17,860
BI18-12-12-12	10,400	5,200	5,200	18,000	22,410
BI18-18-8-23	6,600	3,300	4,950	16,930	20,930
BI18-18-9-14	8,200	4,100	6,150	21,190	26,230
BI18-18-10-11	7,500	3,750	5,625	19,510	24,320
BI18-18-11-13	7,700	3,850	5,775	19,980	24,850
BI18-18-12-12	7,050	3,025	4,538	15,710	19,560
BI18-24-8-23	4,950	2,475	4,950	16,930	29,930
BI18-24-9-14	6,600	3,300	6,600	22,740	28,150
BI18-24-10-11	6,300	3,150	6,300	21,850	27,240
BI18-24-11-13	5,700	2,850	5,700	19,720	24,520
BI18-24-12-12	6,850	3,425	6,850	23,720	29,520
BI18-34-8-23	3,150	1,575	4,462	15,260	18,870
BI18-34-9-14	5,300	2,650	7,508	25,870	32,020
BI18-34-10-11	5,300	2,650	7,508	26,040	32,470
BI18-34-11-13	4,700	2,350	6,658	23,030	28,640
BI18-34-12-12	5,050	2,525	7,403	25,630	31,900
<u>22-gage</u>					
BI22-12-8-12	8,700	4,350	4,350	26,480	30,050
BI22-12-9-16	8,700	4,350	4,350	26,450	31,860
BI22-12-10-15	8,250	4,125	4,125	25,190	30,460
BI22-12-11-13	7,800	3,900	3,900	23,800	28,760
BI22-12-12-11	8,000	4,000	4,000	24,430	29,540
BI22-18-8-14	5,650	2,825	4,238	25,800	29,280
BI22-18-9-16	6,700	3,350	5,025	30,544	36,800
BI22-18-10-14	5,600	2,800	4,200	25,650	31,010
BI22-18-11-13	6,000	3,000	4,500	27,460	33,180
BI22-18-12-11	5,200	2,600	3,900	23,820	28,800
BI22-24-8-14	4,000	2,000	4,000	24,350	27,630
BI22-24-9-20	4,700	2,350	4,700	28,540	34,360
BI22-24-10-14	4,150	2,075	4,150	25,340	30,640
BI22-24-11-13	4,400	2,200	4,400	26,510	32,440
BI22-24-12-11	4,600	2,300	4,600	28,090	33,970

Table 6. Continued

Specimen designation	Ultimate beam load, P_u (lb)	Ultimate shear V_u (lb)	Ultimate moment M_u (ft-lb)	Form stress — psi Centroidal f_{scb}	Bottom f_{sb}
BI22-34-8-23	3,000	1,500	4,250	25,810	31,070
BI22-34-9-20	3,700	1,850	5,241	31,830	38,310
BI22-34-10-14	3,000	1,500	4,250	25,960	31,380
BI22-34-11-13	3,100	1,550	4,391	26,790	32,380
BI22-34-12-11	3,750	1,875	5,312	32,440	36,700
BI22S-12-8-12	5,000	2,500	2,500	15,220	17,270
BI22S-18-9-20	3,400	1,700	2,550	15,490	18,640
BI22S-24-8-12	2,450	1,225	2,450	14,920	16,930
BI22S-34-9-16	2,200	1,100	3,116	18,940	22,820
Averages, not including smooth specimens, for 18-gage and 22-gage					
18-gage					
BI18-12-	9,830	4,915	4,915	16,960	20,670
BI18-18-	7,210	3,605	5,408	18,660	23,180
BI18-24-	6,080	3,040	6,080	20,990	27,870
BI18-34-	4,700	2,350	6,658	23,160	28,780
22-gage					
BI22-12-	8,290	4,145	4,145	25,270	30,130
BI22-18-	5,830	2,915	4,373	26,650	31,810
BI22-24-	4,370	2,185	4,370	26,570	31,810
BI22-34-	3,310	1,655	4,689	28,560	33,970

Table 7. Design and ultimate moment comparisons for beams using 18- and 22-gage steel form I. (See Table 39 in August report.)

Specimen designation	Ultimate experimental moment, M_u (ft-lb)	Calculated design moment, M_{ac} (ft-lb)(a)	Calculated ultimate moment, M_u' (ft-lb)(b)	M_u/M_{ac}	M_u/M_u'	Calculated design moment, M_{ab} (ft-lb)(c)	M_u/M_{ab}
<u>18-gage</u>							
BI18-12-8-23	4,850	5,849	11,928	0.829	0.407	4,730	1.025
BI18-12-9-14	5,100	5,806	11,928	0.878	0.428	4,689	1.088
BI18-12-10-11	5,275	5,766	11,500	0.915	0.459	4,625	1.140
BI18-12-11-13	4,150	5,781	11,622	0.718	0.357	4,649	0.893
BI18-12-12-12	5,200	5,777	11,598	0.900	0.483	4,641	1.120
BI18-18-8-23	4,950	5,849	11,928	0.846	0.415	4,730	1.046
BI18-18-9-14	6,150	5,806	11,928	1.059	0.516	4,689	1.312
BI18-18-10-11	5,625	5,766	11,500	0.976	0.489	4,625	1.216
BI18-18-11-13	5,775	5,781	11,622	0.999	0.497	4,649	1.242
BI18-18-12-12	4,538	5,777	11,598	0.786	0.391	4,641	0.978
BI18-24-8-23	4,950	5,849	11,928	0.846	0.415	4,730	1.046
BI18-24-9-14	6,600	5,806	11,928	1.137	0.553	4,689	1.408
BI18-24-10-11	6,300	5,766	11,500	1.093	0.548	4,625	1.362
BI18-24-11-13	5,700	5,781	11,622	0.986	0.490	4,649	1.226
BI18-24-12-12	6,850	5,777	11,598	1.186	0.591	4,641	1.476
BI18-34-8-23	4,462	5,849	11,928	0.763	0.374	4,730	0.943
BI18-34-9-14	7,508	5,806	11,928	1.293	0.628	4,689	1.601
BI18-34-10-11	7,508	5,766	11,500	1.302	0.653	4,625	1.623
BI18-34-11-13	6,658	5,781	11,622	1.152	0.573	4,649	1.432
BI18-34-12-12	7,403	5,777	11,598	1.281	0.638	4,641	1.595
<u>22-gage</u>							
BI22-12-8-12	4,350	3,284	6,805	1.325	0.635	2,720	1.599
BI22-12-9-16	4,350	3,290	6,861	1.322	0.634	2,731	1.593
BI22-12-10-15	4,125	3,275	6,774	1.260	0.609	2,708	1.523
BI22-12-11-13	3,900	3,278	6,780	1.190	0.575	2,712	1.438
BI22-12-12-11	4,000	3,275	6,774	1.221	0.590	2,708	1.477
BI22-18-8-14	4,238	3,284	6,805	1.290	0.623	2,720	1.558
BI22-18-9-16	5,025	3,290	6,861	1.526	0.732	2,731	1.840
BI22-18-10-14	4,200	3,275	6,774	1.282	0.620	2,708	1.551
BI22-18-11-13	4,500	3,278	6,780	1.373	0.664	2,712	1.659
BI22-18-12-11	3,900	3,275	6,774	1.191	0.576	2,708	1.440

Table 7. Continued

Specimen designation	Ultimate experimental moment, M_u (ft-lb)	Calculated design moment, M_{ac} (ft-lb)(a)	Calculated ultimate moment, M_u' (ft-lb)(b)	M_u/M_{ac}	M_u/M_u'	Calculated design moment, M_{ab} (ft-lb)(c)	M_u/M_{ab}
BI22-24-8-14	4,000	3,284	6,805	1.218	0.588	2,720	1.470
BI22-24-9-20	4,700	3,293	6,881	1.427	0.683	2,736	1.718
BI22-24-10-14	4,150	3,275	6,774	1.267	0.613	2,708	1.532
BI22-24-11-13	4,400	3,278	6,780	1.342	0.649	2,712	1.622
BI22-24-12-11	4,600	3,275	6,774	1.404	0.679	2,708	1.699
BI22-34-8-23	4,250	3,294	6,874	1.290	0.618	2,736	1.553
BI22-34-9-20	5,241	3,293	6,881	1.592	0.762	2,736	1.916
BI22-34-10-14	4,250	3,275	6,774	1.298	0.627	2,708	1.569
BI22-34-11-13	4,391	3,278	6,780	1.340	0.648	2,712	1.619
BI22-34-12-11	5,312	3,275	6,774	1.622	0.784	2,708	1.692
BI22S-12-8-12	2,500	3,284	6,805	0.761	0.367	2,720	0.919
BI22S-18-9-20	2,550	3,293	6,881	0.774	0.370	2,736	0.932
BI22S-24-8-12	2,450	3,284	6,805	0.746	0.360	2,720	0.901
BI22S-34-9-16	3,116	3,290	6,861	0.947	0.454	2,731	1.141
Averages (without smooth forms)							
BI18-12	4,915	5,796	11,715	0.848	0.420	4,667	1.053
BI18-18	5,408	5,796	11,715	0.933	0.462	4,667	1.159
BI18-24	6,080	5,796	11,715	1.074	0.519	4,667	1.303
BI18-34	6,709	5,796	11,715	1.158	0.573	4,667	1.438
BI22-12	4,145	3,280	6,799	1.264	0.610	2,716	1.526
BI22-18	4,373	3,280	6,799	1.333	0.643	2,716	1.610
BI22-24	4,370	3,281	6,803	1.332	0.642	2,717	1.608
BI22-34	4,689	3,283	6,817	1.448	0.688	2,720	1.724

(a) $M_{ac} = f_s I_T/12\ nc_{sb}$, where $f_s = 20{,}000$ psi.

(b) $M_u' = A_s f_y(d - a/2)$ for depth, d, to centroidal axis of the steel form and for $f_y = 40{,}600$ psi.

(c) $M_{ab} = f_s I_T/12\ nc_{sb}$, where $f_s = 20{,}000$ psi.

Table 8. Experimental and design mechanical bond comparisons for beams. (See Table 38 in August report.)

Specimen designation	Ultimate load $- P_u$ (lb)	Ultimate experimental shear, V_u (lb)	Ultimate bond, u_b (psi)	Ultimate bond, u_b' (psi)	Allowable design bond, u_a (psi)	Ratio u_b/u_a	u_b'/u_a
18-gage							
BI18-12-8-23	9,700	4,850	70.50	290.96	40	1.937	7.274
BI18-12-9-14	10,200	5,100	81.34	305.40	40	2.034	7.635
BI18-12-10-11	10,550	5,275	84.82	318.48	40	2.121	7.962
BI18-12-11-13	8,300	4,150	66.54	249.83	40	1.664	6.246
BI18-12-12-12	10,400	5,200	83.09	311.96	40	2.077	7.799
BI18-18-8-23	6,600	3,300	52.73	197.98	40	1.318	4.950
BI18-18-9-14	8,200	4,100	65.39	245.52	40	1.635	6.138
BI18-18-10-11	7,500	3,750	60.30	226.41	40	1.508	5.660
BI18-18-11-13	7,700	3,850	61.73	231.78	40	1.543	5.796
BI18-18-12-12	7,050	3,025	48.34	181.48	40	1.209	4.537
BI18-24-8-23	4,950	2,475	39.55	148.48	40	0.989	3.712
BI18-24-9-14	6,600	3,300	52.63	197.61	40	1.316	4.940
BI18-24-10-11	6,300	3,150	50.65	190.18	40	1.266	4.755
BI18-24-11-13	5,700	2,850	45.69	171.57	40	1.142	4.289
BI18-24-12-12	6,850	3,425	54.727	205.48	40	1.368	5.137
BI18-34-8-23	3,150	1.575	25.16	94.49	40	0.629	2.362
BI18-34-9-14	5,300	2,650	42.26	158.69	40	1.057	3.967
BI18-34-10-11	5,300	2,650	42.61	159.99	40	1.065	3.999
BI18-34-11-13	4,700	2,350	37.68	141.47	40	0.942	3.537
BI18-34-12-12	5,050	2,525	40.35	151.48	40	1.009	3.787
22-gage							
BI22-12-8-12	8,700	4,350	67.26	252.53	40	1.682	6.313
BI22-12-9-16	8,700	4,350	67.06	251.77	40	1.677	6.294
BI22-12-10-15	8,250	4,125	63.92	239.97	40	1.598	5.999
BI22-12-11-13	7,800	3,900	60.38	226.71	40	1.510	5.668
BI22-12-12-11	8,000	4,000	61.98	232.70	40	1.550	5.818
BI22-18-8-14	5,650	2,825	43.68	163.99	40	1.092	4.099
BI22-18-9-16	6,700	3,350	51.64	193.90	40	1.291	4.848
BI22-18-10-14	5,600	2,800	43.39	162.89	40	1.085	4.072
BI22-18-11-13	6,000	3,000	46.45	174.39	40	1.161	4.360
BI22-18-12-11	5,200	2,600	40.29	151.26	40	1.007	3.782
BI22-24-8-14	4,000	2,000	30.92	116.10	40	0.773	2.903
BI22-24-9-20	4,700	2,350	36.17	135.81	40	0.904	3.395
BI22-24-10-14	4,150	2,075	32.15	120.71	40	0.804	3.018
BI22-24-11-13	4,400	2,200	34.06	127.89	40	0.852	3.197
BI22-24-12-11	4,600	2,300	35.64	133.80	40	0.891	3.345
BI22-34-8-23	3,000	1,500	23.19	86.70	40	0.580	2.168
BI22-34-9-20	3,700	1,850	28.48	106.91	40	0.712	2.673
BI22-34-10-14	3,000	1,500	23.24	87.26	40	0.581	2.182
BI22-34-11-13	3,100	1,550	23.99	90.10	40	0.600	2.253
BI22-34-12-11	3,750	1,875	29.05	109.08	40	0.726	2.727
BI22S-12-8-12	5,000	2,500	38.65		40	0.966	
BI22S-18-9-20	3,400	1,700	26.16		40	0.654	
BI22S-24-8-12	2,450	1,225	18.94		40	0.474	
BI22S-34-9-16	2,200	1,100	16.96		40	0.424	
Averages							
BI18-12	9.830	4,915	78.66	295.33	40	1.967	7.383
BI18-18	7,210	3,605	57.70	216.63	40	1.443	5.416
BI18-24	6,080	3,040	48.65	182.45	40	1.216	4.567
BI18-34	4,700	2,350	39.74	141.22	40	0.940	3,530
BI22-12	8,290	4,145	64.12	240.74	40	1.603	6.018
BI22-18	5,830	2,915	45.09	169.27	40	1.127	4.232
BI22-24	4,370	2,185	33.79	126.86	40	0.845	3.172
BI22-34	3,310	1,655	25.59	96.01	40	0.640	2.401

Table 9. Experimental results for pushout tests. (See Tables 4 and 8 in August report.)

Specimen designation	Jack load — P'_u (lb)	Form load, F_u (lb)	Form stress, f_{scp} (psi)	Area — in.^{2}		Mechanical bond stress[b] — psi	
				$L'\Sigma'_o$	$L'\Sigma_o$	Effective, u'_p	Total, u_p
18-gage							
VI18-12-8-11	19,600	9,800	11,086	52.8	198.2	185.6	49.4
VI18-12-9-16	23,200	11,600	13,122	52.8	198.2	219.7	58.5
VI18-12-10-11	15,500	7,750	8,767	52.8	198.2	146.8	39.1
VI18-12-11-11	19,600	9,800	11,085	52.8	198.2	185.6	49.4
VI18-12-12-10	22,200	11,100	12,540	52.8	198.2	210.2	56.0
VI18-18-8-11	20,600	10,300	11,652	79.2	297.4	130.0	34.6
VI18-18-9-16	19,900	9,950	11,256	79.2	297.4	125.6	33.4
VI18-18-10-11	19,100	9,550	10,803	79.2	297.4	120.6	32.1
VI18-18-11-11	22,200	11,100	12,557	79.2	297.4	140.2	37.3
VI18-18-12-10	22,900	11,450	12,952	79.2	297.4	144.6	38.5
VI18-24-8-11	21,700	10,850	12,274	105.6	396.5	102.7	26.7
VI18-24-9-16	21,700	10,850	12,274	105.6	396.5	102.7	26.7
VI18-24-10-11	18,600	9,300	10,520	105.6	396.5	88.1	23.4
VI18-24-11-11	18,300	9,150	10,351	105.6	396.5	86.6	23.1
VI18-24-12-10	26,800	13,400	15,158	105.6	396.5	126.9	33.8
VI18-34-8-11	24,200	12,100	13,688	149.6	561.7	80.9	21.5
VI18-34-9-16	23,700	11,850	13,405	149.6	561.7	79.2	21.1
VI18-34-10-11	21,100	10,550	11,934	149.6	561.7	70.5	18.8
VI18-34-11-11	21,700	10,850	12,274	149.6	561.7	72.5	19.3
VI18-34-12-10	29,400	14,700	16,629	149.6	561.7	98.3	26.2
22-gage							
VI22-12-8-11	16,000	8,000	16,427	52.8	198.2	151.5	40.4
VI22-12-9-16	16,800	8,400	17,248	52.8	198.2	159.1	42.4
VI22-12-10-10	14,200	7,100	14,579	52.8	198.2	134.5	35.8
VI22-12-11-11	14,500	7,250	14,887	52.8	198.2	137.3	36.6
VI22-12-12-10	16,500	8,250	16,940	52.8	198.2	156.2	41.6
VI22-18-8-11	14,000	7,000	14,374	79.2	297.4	88.4	23.5
VI22-18-9-16	16,000	8,000	16,427	79.2	297.4	101.0	26.9
VI22-18-10-11	15,000	7,500	15,400	79.2	297.4	94.7	25.2
VI22-18-11-11	16,500	8,250	16,940	79.2	297.4	104.16	27.7
VI22-18-12-10	19,100	9,550	19,610	79.2	297.4	120.6	32.1
VI22-24-8-11	18,100	9,050	18,583	105.6	396.5	85.7	22.8
VI22-24-9-16	18,100	9,050	18,583	105.6	396.5	85.7	22.8
VI22-24-10-10	15,800	7,900	16,222	105.6	396.5	74.8	19.9
VI22-24-11-11	16,200	8,100	16,632	105.6	396.5	76.7	20.4
VI22-24-12-10	17,000	8,500	17,454	105.6	396.5	80.5	21.4
VI22-34-8-11	17,600	8,800	18,070	149.6	561.7	58.8	15.7
VI22-34-9-16	18,300	9,150	18,788	149.6	561.7	61.2	16.3
VI22-34-10-10	15,000	7,500	15,400	149.6	561.7	50.1	13.4
VI22-34-11-11	18,300	9,150	18,788	149.6	561.7	61.2	16.3
VI22-34-12-10	18,500	9,250	18,994	149.6	561.7	61.8	16.5
Averages							
VI18-12	20,020	10,010	11,323	52.8	198.2	189.7	50.5
VI18-18	20,940	10,470	11,844	79.2	297.4	132.3	35.2
VI18-24	21,420	10,710	12,115	105.6	396.5	101.4	26.7
VI18-34	24,020	12,010	13,586	149.6	561.7	80.6	21.4
VI22-12	15,600	7,800	16,016	52.8	198.2	147.7	39.4
VI22-18	16,120	8,060	16,550	79.2	297.4	101.8	27.1
VI22-24	17,040	8,520	17,495	105.6	396.5	80.7	21.5
VI22-34	17,540	8,770	18,008	149.6	561.7	58.6	15.6

[a] All specimens tabulated here were tested on the bottom block with the top block clamped.

[b] Bond stress based on formulas: $u'_p = F_u/\Sigma'_o L'$, where F_u is form load and $\Sigma'_o L'$ is the effective surface area of steel form; $u_p = F_u/\Sigma_o L'$, where $\Sigma_o L'$ is the total surface area of steel form.

Table 10. Experimental correlation of pushout tests to beam tests. (See Table 33 in August report.)

Steel gage	Length — L' (in.)	Ultimate form stress[b] — f_{scb} (beam) (psi)	Ultimate form stress — f_{scp} (pushout) (psi)	Ratio f_{scp}/f_{scb} $R_{f_{sc}}$	Ultimate mechanical bond[c] — u_b (beam) (psi)	Ultimate mechanical bond — u_p (pushout) (psi)	Ratio u_p/u_b R_u
18	12	16,962 (5)[a]	11,320 (5)	0.667	78.66	50.5	0.642
18	18	18,662 (5)	11,844 (5)	0.635	57.70	35.2	0.610
18	24	20.989 (5)	12,115 (5)	0.577	48.65	26.1	0.536
18	34	23,165 (5)	13,586 (5)	0.586	37.61	21.4	0.569
22	12	25,267 (5)	16,016 (5)	0.634	64.12	39.4	0.614
22	18	26.653 (5)	16,550 (5)	0.621	45.09	27.1	0.601
22	24	26,568 (5)	17,495 (5)	0.658	33.79	21.5	0.636
22	34	28.564 (5)	18,008 (5)	0.630	25.59	15.6	0.610

[a] Number in parentheses indicates the number of tests from which the average value listed was obtained.

[b] Values pertain to average stress at centroidal axis of the form.

[c] Values obtained from $u = V_u/\Sigma_o jd$ based on a depth to centroidal axis of the form.